REGULATORY T CELL DERIVED EXTRACELLULAR VESICLES – DESIGNING NOVEL IMMUNE BASED THERAPIES TO PROLONG THE LIFESPAN OF TRANSPLANTED TISSUE

JORDAN JULICIEN BAZOER

A thesis submitted in fulfilment of the requirements of the University of East London for the degree of Master of Research in Bioscience

May 2022

Acknowledgements

I would like to start by showing my gratitude to Dr Lesley Smyth, firstly for the opportunity to collaborate with her on this project and secondly for all the support and understanding throughout the turbulent times during my Mres. I cannot thank her enough for her guidance and motivation, which gave me the strength I needed to see this project through.

I would like to thank Dr Marco Romano and Adeel Saleem, who were kind enough to provide some key reagents and cell lines, allowing this research to be carried out. Without them, this research would not be possible.

I would like to thank Professor Lombardi for her collaborative efforts in this project, allowing the use of key reagents and cell lines as well as equipment.

I would also like to thank the PGR students at UEL, who have formed a community of support amongst them that uplifts and motivates all of us.

Finally, I would like to thank my family for their continued support throughout my work and their backing which gave me the confidence I needed to complete this MRes.

Table of Contents

Acknowledgements ***2***

List of Figures ***5***

Abbreviations ***6***

Abstract ***8***

Introduction ***9***

Regulatory T cells **9**

Regulatory T cells in Tolerance **10**

Antigen-specific Regulatory T cells **12**

Regulatory T cell function **15**

Regulatory T cell Extracellular Vesicles (EVs) **16**

Regulatory T cell EVs **17**

Therapeutic Potential of Regulatory T cell EVs **18**

Targeting EVs **19**

Aim and Objectives **22**

Materials and Methods ***23***

Reagents and Solutions **23**

Centrifugation **23**

Cell Lines **23**

Media **23**

Treg and CAR-Treg Line Expansion **24**

Expanded Treg Phenotyping **24**

EV Isolation **25**

CD81 Treg-EV Validation **26**

Phosphatidylserine (PS) ELISA **27**

X-Stamp Treg-EV decoration **28**

Targeting of Xstamp Pro 'decorated' Treg-EV to B cells. **29**

Validation of CAR expression of CAR-Treg derived EVs **30**

Co-culture of CAR-Treg-EVs with B cells **30**

Statistical analysis **30**

Results ***31***

Characterisation of $CD4^{+}CD25^{+}CD127^{lo}$ Expanded Tregs **31**

Validating CD81 expression of Treg-EVs using an anti-CD81 ELISA. **33**

Confirmation of Phosphatidylserine (PS) expression on Treg-EVs **35**
CFSE-labelling of Tregs **37**
Confirmation of HLA-A2 expression on expanded B cells lines **38**
..... **40**
Treg-EV Acquisition by B cells is mediated via PS. **40**
Post Isolation PS-mediated targeting did not create antigen specific Treg-EVs **43**
Characterisation of expanded HLA-A2 CAR Tregs **45**
..... **47**
Treg-EVs express the HLA-A2 specific CAR **47**
..... **50**
CAR-dependent acquisition of CAR-EVs by HLA-A2 expressing B cells **50**
..... 52
Discussion 53
PS and Treg EV acquisition **53**
Alternative Methods of Post Isolation EV Modifications **57**
Antigen specific Treg EVs as a possible therapeutic reagent **61**
References. 64
Appendix 77
Appendix 1: A table listing the supplier information for the reagents used in this study. **77**
Appendix 2: A table listing the supplier information and clones for the antibodies used in this study. **78**

List of Figures

Figure 2: An illustration of HLA-A2 Specific CAR motif_____12
Figure 4: An illustration of Pre-Isolation and Post-Isolation EV Modification Targets_____17
Figure 5: An illustration of the PS-anchored HLA-A2 targeting motif_____26
Figure 6: Confirmation of Treg-associated markers_____29
Figure 7: Validating CD81 expression on Treg-EVs_____30
Figure 8: Validating the expression of PS on Treg-EVs_____32
Figure 9: Confirmation of CFSE staining of Expanded Tregs_____34
Figure 10: Confirmation of HLA-A2 expression of B cells_____36
Figure 11: CFSE Acquisition of HLA-A2- B cells post-incubation with naïve and targeted Treg-EVs_____38
Figure 12: CFSE Acquisition of HLA-A2+ B cells post-incubation with naïve and targeted Treg-EVs_____40
Figure 13Confirmation of Treg-associated markers on CAR Tregs_____42
Figure 14: Confirmation of successful CD81 Capture of Treg-EVs using CD81 beads____44
Figure 15: Validation of CAR expression on Treg-EVs_____45
Figure 16: CFSE Acquisition of CAR-EVs by HLA-A2- and HLA-A2+ B cells_____47

Abbreviations

AMP – Adenosine Monophosphate
ATP – Adenosine Triphosphate
APC – Antigen Presenting Cell
B cell – B lymphocytes
BCR – B Cell Receptor
BIM – Bcl2 interacting mediator of cell death
Bregs – Regulatory B Cells
BM-DCs – Bone-Marrow Derived Dendritic Cells
BSA – Bovine Serum Albumin
CAR – Chimeric Antigen Receptor
CFSE - Carboxyfluorescein Succinimidyl Ester
CTL- Cytotoxic T Cell
CTLA-4 – Cytotoxic T Lymphocyte Associated Protein 4
DCs – Dendritic Cells
DNA – Deoxyribonucleic Acid
EDTA - Ethylenediaminetetraacetic Acid
EGFR – Epidermal Growth Hormone Receptor
EM- Electron Microscopy
EVs – Extracellular Vesicles
FACS – Fluorescence-activated Cell Sorting
FCS – Foetal Calf Serum
FSC – Forward Scatter
FoxP3 – Forkhead Box P3
GFP – Green Fluorescent Protein
GvHd- Graft-versus-Host Disease
GPI – glycosylphosphatidylinositol
HER2 – Human Epidermal Growth Factor 2
HS – Human Serum
HUVEC – Human Umbilical Cord Endothelial Cells
IBD – Irritable Bowel Syndrome
IFN-γ - Interferon γ
IL-2 – Interleukin 2
IL-10 – Interleukin 10
iNOS – inducible Nitric Oxide Synthase
ISEV – International Society of Extracellular Vesicles
iTregs – Induced Tregs
LAP – Latency Associated Protein
LPS -Lipopolysaccaharide
MFI – Mean Fluorescence Index
miRNA - MicroRNA
MHC- Major Histocompatibility Complex
MST – Microscale Thermophoresis

nTregs – Natural Tregs
NK – Natural Killer Cells
NKT – Natural Killer T Cells
Nrp-1 – Neuropilin 1
NTA – NanoTracking Analysis
PBS – Phosphate Buffered Saline
PBMCs – Peripheral Blood Mononuclear Cells
PS – Phosphatidylserine
PD-L1 – Programmed Death Ligand 1
RAPA – Rapamycin
RNA – Ribonucleic Acid
scFv – Single Chain Variable Fragment
SSC – Side Scatter
Teffs – T Effector cells
TNF-α - Tumor Necrosis Factor alpha
TIM-1 – T Cell Ig and Mucin Domain-Containing Molecule 1
NOD – Nonobese Diabetic
OVA - Ovalbumin
T cell – T Lymphocyte
TCR – T Cell Receptor
TMB – 3,3’,5,5’-Tetramethylbenzidine
Tregs – Regulatory T cell

Abstract

Regulatory T cells (Tregs) are a subpopulation of CD4+ T cells with suppressive capacity and key functions in the regulation of immune responses. Furthermore, Tregs have been shown to secrete extracellular vesicles (EVs) which have been shown to exert similar functions as described by Tregs in a range of settings, including transplantation. Recently, a key study showed the suppressive capacity of human Treg-EVs, albeit not to the extent of Tregs. However, Treg-EVs were able to promote allograft survival in a humanised mouse model. This highlighted the opportunity to investigate whether targeting Treg-EVs pre-isolation and post-isolation could improve their potency. In this study, the efficacy of using these modifications of Treg-EVs to express a HLA-A2 targeting motif was assessed. To investigate post-isolation targeting, first CD81+ Treg-EVs were shown to express phosphatidylserine (PS), forming the surface membrane anchor for the generation of post-isolation modified Treg-EVs. Next, the PS expressed on Treg-EVs was directly conjugated with a linker molecule and subsequently an anti-HLA-A2 antibody, forming the HLA-A2 targeting motif. Interestingly, in comparison to naïve EVs, the acquisition of targeted Treg-EVs by HLA-A2+ B cells was significantly decreased.

Following this, to generate pre-isolation modified EVs, CD81+ EVs were isolated from Chimeric Antigen Receptor (CAR) Tregs. These EVs were shown to express a HLA-A2-specific CAR and were shown to improve acquisition by HLA-A2+ B cells.

These findings demonstrate that the use of pre-isolation modification to express CAR on Treg-EVs improved targeting efficacy while direct conjugation of PS expressed on Treg-EVs may inhibit their acquisition by B cells. Taken together, this study highlights the potential of the use of CAR-EVs as a non-cellular therapeutic to promote allograft survival. Furthermore, this study forms the basis for further investigation into the potential uses of inhibited Treg-EV acquisition via PS-conjugation, particularly in a cancer setting.

Introduction

Regulatory T cells

Cellular therapy has been at the forefront of literature in the search of immunomodulatory therapies for several pathologies (add references). Particularly, T-lymphocytes (T cells) have generated the significant research interest with the potential adaptability of T cells for use in different settings. Regulatory T cells (Tregs), a subset of CD4+ T cells, are increasingly becoming of interest in this field as they have been shown to regulate immune responses through the act of immunosuppression as reviewed by Okeke and Uzonna, (2019). Tregs are separated into two subtypes: natural (nTregs) which develop in the thymus and induced Tregs (iTregs) which develop in the periphery (Mikami *et al.*, 2020) as shown in Figure 1. During the selection process of T cell development in the thymus, thymocytes that are reactive to self-antigen presented via self-Major Histocompatibility Complex II (MHC-II) differentiate into Forkhead box $P3^{+}$ (FoxP3+) T cells and give rise to nTregs as reviewed by Bettini and Vignali, (2010). iTregs however, develop when naive T cells encounter antigen stimulation in the periphery causing them to differentiate into a regulatory state as reviewed by Kanamori *et al.*, (2016).

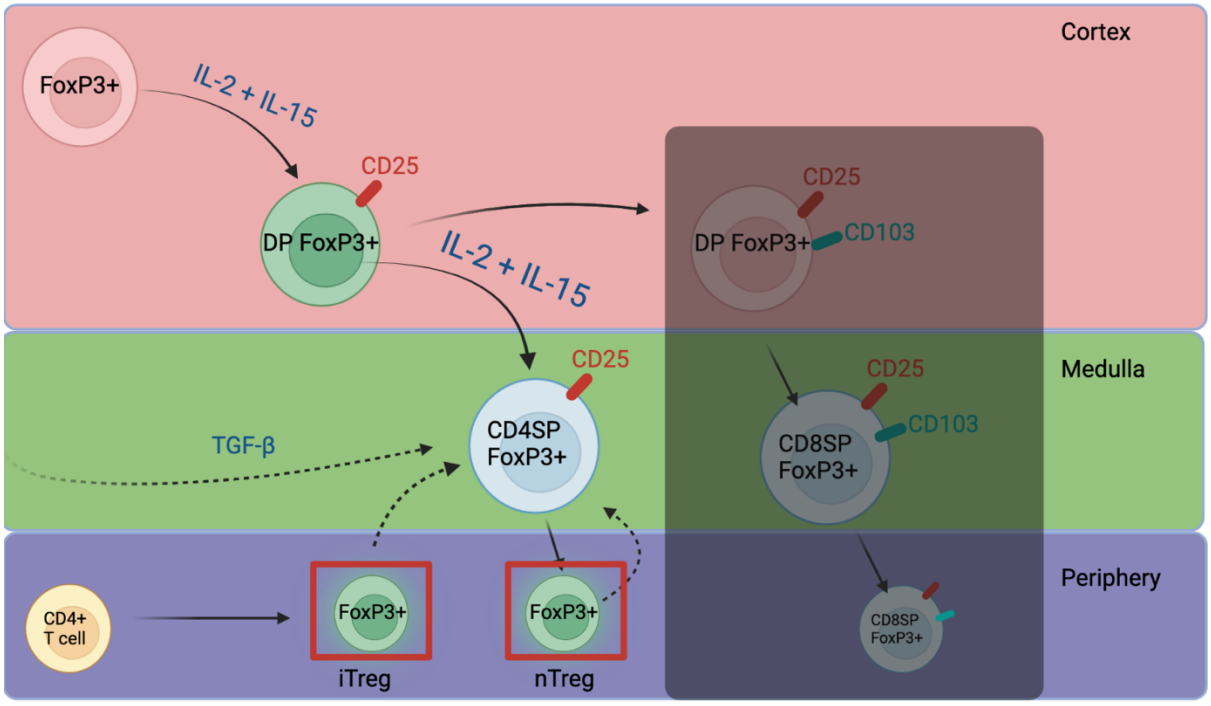

Figure 1: A simple overview of the developmental process of natural CD4+ Tregs and the spontaneous development of iTregs post antigen stimulation in the periphery.

Murine Tregs are typically characterised by the expression of CD25 and the transcription factor, Forkhead box P3 (FoxP3) (Hori, Nomura and Sakaguchi, 2003), both of which are closely involved in the desirable immunosuppressive property of Tregs (R.Walker *et al.*, 2003; Pillai *et al.*, 2007). The characterisation of human Tregs however, has not yet been clearly defined with specific marker expression and are generally distinguished by the $CD4^{+}CD25^{+}CD127^{low}$ phenotype. Recently, Lam *et al.*, (2022) have proposed Helios to be a potential marker of human Treg stability in vitro. Murine Tregs are able to suppress the function of immune cells such as: NK cells (Barao *et al.*, 2006), B cells (Xu *et al.*, 2016), Dendritic cells (DCs) (Tung *et al.*, 2018), as well as effector T cells (Teffs) (Dowling *et al.*, 2018). Human Tregs also suppress the function of immune cells such as: B cells (Lim *et al.*, 2005), NKT cells (Azuma *et al.*, 2003), DCs (Fassbender *et al.*, 2010) and Teffs (Ye *et al.*, 2012).

Regulatory T cells in Tolerance

The continued understanding of Treg biology has led to increased interest into the potential use of Tregs in autoimmunity as a novel immunotherapy. Early research by Tang *et al.*, (2004) elucidated the potential of Tregs in a diabetes setting using a nonobsese diabetic (NOD) mouse model. These authors were able to show the long-term survival and proliferation of ex vivo expanded functional murine Tregs that were able to suppress and prevent the onset of diabetes for up to 20 weeks. Tang *et al* also showed that when used concurrently with a islet transplantation, adoptive transfer of ex vivo expanded Tregs could reverse the diabetic state of the NOD mice through the promotion of islet graft tolerance. Furthermore, phase I clinical trial data (NCT02772679) by a group led by Tang, showed the safe reinfusion of autologous ex vivo expanded functional polyclonal Tregs to treat Type 1 diabetes (Bluestone *et al.*, 2015). Phase I clinical trials are also underway to investigate the safety of using high doses of ex vivo expanded Tregs to treat adults with treatment-resistant Guillain-Barre Syndrome (NCT03773328). Other clinical trials are also investigating the safety of using ex vivo expanded Tregs therapeutically in autoimmune hepatitis (NCT02704338), pemphigus (NCT03239470), lupus (NCT02428309) and ulcerative colitis (NCT04691232).

Similarly, Tregs have been shown to play an important role in the prevention of acute and chronic allograft rejection using preclinical animal models including mice (Onishi *et al.*, 2008; Campos-Mora *et al.*, 2019). Camps-Mora *et al.,* (2019) used a murine skin transplant model to show the importance of Treg-expressed Neuropilin-1 (Nrp1) in the promotion of allograft tolerance through the promotion of the release of anti-inflammatory cytokines such as IL-10 as well as inhibiting the proliferation of T effector cells (Teffs). Onishi *et al.*, (2008) instead showed the aggregation of murine Tregs around Dendritic cells (DCs) and the induction of CD80/86 downregulation in DCs, both of which prevent their ability to activate antigen-reactive T cells.

The successes of Tregs in preclinical studies have led to clinical trials using ex vivo expanded Tregs to induce tolerance (Sawitzki *et al.*, 2020; Sánchez-Fueyo *et al.*, 2020; Harden *et al.*, 2021; Brook *et al.*, 2022). One such clinical trial was the ONE Study (NCT02091232) where donor and recipient cells were mixed with belatacept ex vivo, Tregs sorted and reinfused into the recipient to induce tolerance. The study found that the reinfusion of Tregs was safe, however, the treatment was not able to induce long-lasting tolerance. Todo *et al.*, (2016) carried out a similar clinical trial where ex-vivo expanded Treg-enriched cell suspension was reinfused into patients to promote tolerance and allow for the weaning of immunosuppressive medication from 6 months post-reinfusion. Although two cases of rejection were observed, the study found that patients could successfully be weaned off immunosuppressants, as the rejection was mitigated with the reintroduction of immunosuppressants. Harden *et al.*, (2021) conducted a phase I clinical trial which investigated the efficacy and safety of ex vivo expanded autologous polyclonal Tregs used in instead of induction therapy to prevent acute transplant rejection and further decreasing the load of immunosuppressants. The trial data shows that allograft survival remained at 100% for up to 48 months in the control group and the experimental group who received Treg therapy. Interestingly, the Treg therapy group experienced a lower rate of acute rejection and the allograft survived without the need for induction therapy assumed to be due to the persistence of infused Tregs in the periphery.

Similarly, Sánchez-Fueyo *et al.*, (2020) presented data from the first in-human phase I trial investigating the efficacy and safety of infusing ex vivo expanded autologous polyclonal Tregs into liver transplant patients, 6-12 months post-transplant. The study showed that only one out the six patients who received the infusion of the Tregs experienced adverse effects due to Treg infusion at a concentration of $4.5x10^6$ Tregs/kg.

The therapy was otherwise deemed safe and was shown to decrease immune responses to donor-type cells, assumed to be attributed to the upregulation of CD154 on CD8+ memory T cells. In total, 14 studies that are investigating the potential and safety of using Tregs to induce tolerance have been completed and another 15 recruiting, not yet recruiting or active, not recruiting according to clinical trial data from ClinicalTrials.gov.

Early research into the in vitro and in vivo effects and general potential of Tregs relied on the use of a heterogenous population of polyclonal Tregs. However, more recent research using murine models have shown that 'targeted' Tregs with direct antigen specificity were more efficacious than their polyclonal counterparts in diabetes (Tang *et al.*, 2004; Tarbell *et al.*, 2004), gastritis (DiPaolo *et al.*, 2007), multiple sclerosis (Stephens, Malpass and Anderton, 2009) graft-versus host disease (GvHD (Trenado *et al.*, 2003) and transplantation (Golshayan *et al.*, 2007; Joffre *et al.*, 2008; Tsang *et al.*, 2008; Yuen-Shan Tsang *et al.*, 2009; Sagoo *et al.*, 2011).

Antigen-specific Regulatory T cells

The potential of Tregs in the clinical setting has gained interest recently due to the increased knowledge and ease of genetic modifications of cells as reviewed by Amini *et al.*, (2021). The generation of adaptable transduction techniques as well as the possibility of using proteomic screening to highlight unique target molecules on the target cell of interest has made it possible to develop 'targeted' Tregs, shown to be more potent than polyclonal Tregs (Putnam *et al.*, 2013). These technologies may help decrease the number of Tregs needed to induce the functional response wanted as well as prevent possible off-target immunosuppression. This also reduces the need for extensive ex vivo expansion of Tregs for therapeutic use; thus preventing the reduction in suppressive capacity by repeated stimulation and expansion of human Tregs, as described by Hippen *et al.*, (2011).

One way to engineer antigen-specific Tregs is through genetic modification of the T cell receptor (TCR) using lentiviral or retroviral transduction as shown by Kato *et al.*, (2008), Kim *et al.*, (2015) & Campos-Mora *et al.*, (2019) and these cells have been shown to be superior in function in comparison to polyclonal Tregs (Putnam *et al.*, 2013). For example, using a mismatched mouse skin transplant model and a fully mismatched mouse heart transplant model, Tsang *et al.*, (2008) showed that Tregs expressing a transduced TCR, with

specificity for the alloantigen and daily rapamycin was able to induce allograft survival for up to 150 days and resulted in better histological outcomes in comparison to self-reactive Treg treatment.

Another targeting technique adopted to increase target specificity of cells is using chimeric antigen receptors (CARs) as shown by MacDonald *et al.*, (2016), Boardman *et al.*, (2017), Noyan *et al.*, (2017) & Boroughs *et al.*, (2019). CARs are receptors which are composed of a scFv section, a transmembrane portion, a signalling domain and typically a fluorescent tag as shown in Figure 2.

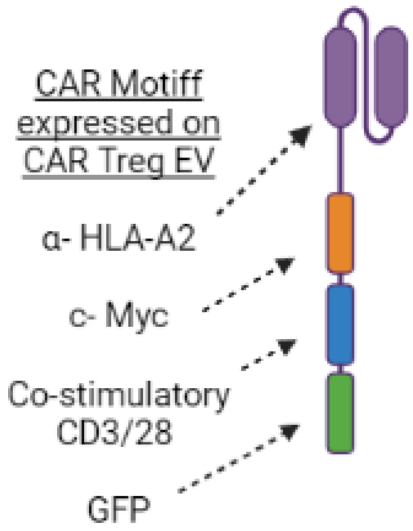

Figure 2*:* An illustrative diagram depicting the components of a HLA-A2 specific CAR motif.

The scFv component is the portion of the CAR which recognises the antigen and is usually derived from an antibody which recognises a specific marker protein on the target cell. Unlike TCR, the CAR does not require MHC-matched expression of peptides or peptide processing for it to be recognised, thus leading to an increase in the number of individual targets of the CAR expressing cells (Sadelain, Brentjens and Rivière, 2013). A study by MacDonald *et al.*, (2016) has also shown that activation of human Tregs via the CAR rather than the TCR results in increased upregulation of Treg function-associated proteins such as Cytotoxic T Lymphocyte Associated Protein 4 (CTLA-4), latency-associated peptide (LAP) and glycoprotein.

CAR-Treg cells have been shown to be successful in preclinical models where they induce transplant tolerance better than polyclonal Tregs. Boardman et al., (2017) used an HLA-A2 specific scFv sequence to generate a CAR that was successfully expressed on the surface of Tregs without affecting functionality. The HLA-A2 specific scFv allowed for increased binding specificity of Tregs to HLA-A2 expressing cells. Furthermore, the study showed that these CAR-Tregs were significantly more suppressive than non-transduced Tregs producing more IL-10, an immunosuppressive cytokine, than the latter. Boardman *et al.*, (2017) were the first to show the potential of CAR-Tregs in a transplant setting. Using a humanised mouse skin transplant model, the study showed that the injection of CAR-Tregs into mice led to the inhibition of alloimmune-mediated injury of the skin graft. This inhibition was also found to be superior to that of polyclonal Tregs.

This group further showed the potent immunosuppressive capability of CAR-Tregs through the co-expression of IL-10 along with the CAR motif (Mohseni *et al.*, 2021). IL-10 and HLA-A2 CAR expressing Tregs were shown to enhance the suppressive effects previously shown by Tregs which only expressed the HLA-A2 targeting motif.

Using a humanised mouse skin transplant model, Noyan *et al.*, (2017) also showed the ability to generate functional HLA-A2-CAR Tregs possessing the ability to almost completely inhibit alloimmune reaction in vivo as well as protect the allograft from alloimmune injury. MacDonald *et al.*, (2016) also used a mouse model to show superior interaction of HLA-A2 CAR Tregs with their target HLA-A2 expressing cells in comparison to polyclonal Tregs in a Graft versus Host Disease (GvHD).

A study by Sicard *et al.*, (2020) has demonstrated that the use of HLA-A2 specific CAR-Tregs, but not irrelevant HER2 specific CAR-Tregs, promoted allograft survival *in vivo* through the inhibition of B cells and their secretion of donor-specific antibodies using a mouse skin transplant model. However, HLA-A2 specific CAR-Tregs were not able to promote allograft survival in sensitised mice, suggesting that their adoptive transfer does not inhibit memory alloreactivity.

Regulatory T cell function

The immunosuppressive capabilities of Tregs have made them a good clinical therapeutic to promote tolerance, as previously mentioned. However, despite the success little is known about their mechanism of action in vivo. More research input into this area is required to elucidate how best to harness the true potential of Tregs for therapeutic use. One way that Tregs have been shown to exert their suppressive properties is through the expression of cytotoxic T lymphocyte-associated antigen 4 (CTLA-4) which gives Tregs the ability to trogocytose CD80/86 present on dendritic cells (DCs) and thus inducing an increase in free programmed-death ligand-1 (PD-L1) (Tekguc *et al.*, 2021). This then inhibits the stimulation of T cells by DCs, thus dampening immune responses. Furthermore, a recent study by Akkaya *et al.*, (2019) showed that murine Tregs also have the ability to trogocytose MHC Class II molecules from the surface of DCs. This lead to a down-regulation of antigen-presentation by DCs to Teffs, thus decreasing T cell-led immune responses.

The interplay between Tregs and Teffs has been highlighted in literature because of its importance in achieving a tolerogenic state. For example, using a mouse model, Onishi *et al.*, (2008) showed that murine Tregs out-performed OVA-specific Teffs by aggregating around OVA-pulsed DCs, thus inhibiting the Teff-DC interaction.

Thornton and Shevach, (1998) also showed that the CD25 expression on Tregs aided in their suppressive effects through its antagonistic binding of Interleukin 2 (IL-2), thus preventing the stability of Teffs through the induction of apoptosis via the Bcl2 interacting mediator of cell death (BIM) signalling pathway, as described by Pandiyan *et al.*, (2007). Tregs can also induce apoptosis through the production of granzymes A and B, as well as perforin, which is believed to induce the BIM apoptosis pathway (Gondek *et al.*, 2005). The conversion of Adenosine Triphosphate (ATP) into extracellular adenosine by CD39 and CD73 expressed on the cell surface of Tregs highlights another mechanism believed to be important in suppressive capacity, as the converted adenosine has been shown to inhibit the secretion of IL-12 and TNF-α from Antigen Presenting cells (APCs) and inhibit IL-2, Interleukin 4 (IL-4), Interferon γ (IFN-γ) and Tumor Necrosis Factor α (TNF-α) release from T helper cells, as reviewed by Ernst, Garrison and Thompson, (2010). Membrane-bound and soluble inhibitory cytokines have also been implicated. Collison *et al.*, (2009), using a transwell method, showed that Treg were able to suppress proliferation of Teffs through contact-independent means via Interleukin 10 (IL-10) and Interleukin 35 (IL-35), which directly opposes earlier

studies which suggested Treg suppression occurred in an IL-10 and IL-35-independent manner (Takahashi *et al.*, 1998; Thornton and Shevach, 1998; Jonuleit *et al.*, 2001).

Extracellular Vesicles (EVs)

EVs is an umbrella term used to describe nano-sized lipid membrane vesicles (Théry *et al.*, 2018) that are released by a number of different cells including, but not limited to, B cells (Raposo and Stoorvogel, 2013; Saunderson *et al.*, 2014), DCs (Zitvogel *et al.*, 1998), endothelial cells (Van Niel *et al.*, 2001), mesenchymal stem cells (Yeo *et al.*, 2013; Shigemoto-Kuroda *et al.*, 2017), cancer cells (Wolfers *et al.*, 2001) and T cells (Blanchard *et al.*, 2002), including Tregs (Chaput, 2006; Lesley Ann Smyth *et al.*, 2013; Aiello *et al.*, 2017; Tung *et al.*, 2018). EVs can be broken down into three main groups: exosomes, microvesicles and apoptotic bodies which are differentiated by size, membrane composition, contents, site of biogenesis and function (Zaborowski *et al.*, 2015; Oggero, Austin-Williams and Norling, 2019). As reviewed by Doyle and Wang, (2019), exosomes are small 30-150nm endosomal vesicles which are thought to be secreted by all cell types, microvesicles are larger 100nm-1µm vesicles formed through outward budding of the plasma membrane, apoptotic bodies often being the largest with a size ranging 50nm-5000nm in diameter as depicted in Figure 3.

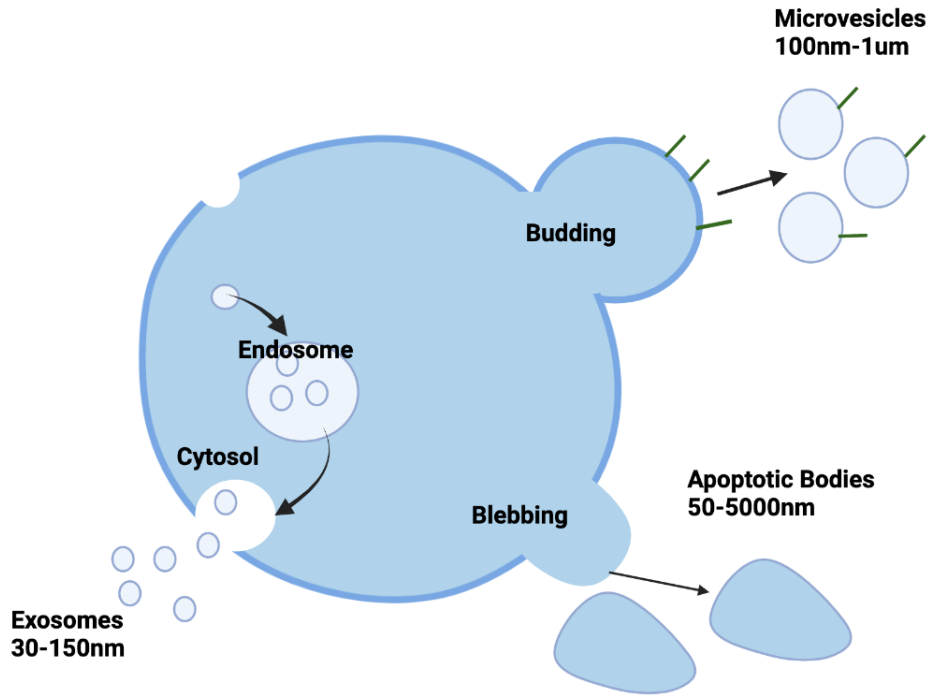

Figure 3: A simple depiction of the biogenesis and size of the three main subtypes of EVs: exosomes, microvesicles and apoptotic bodies.

Apoptotic bodies are secreted into the extracellular space by dying cells (Kakarla *et al.*, 2020). Distinctions between the EV subtypes are important to help elucidate specific functions that can be attributed to each subtype. However, due to the heterogeneity of most EV samples and the lack of distinct markers, characterisation of an EV subtype has been difficult. However, recent studies have postulated that ALIX and Tsg101, may be markers of the exosome as shown by Sette *et al.*, (2010) & Colombo *et al.*, (2013).

EVs have been shown to contain biological molecules including membrane proteins, lipids, Ribonucleic Acid (RNA) and Deoxyribonucleic Acid (DNA) which can be transported to other cells, creating an indirect cell-to-cell communication system which allows the movement of biological material between cells (Zhang et al., 2019).

Regulatory T cell EVs

Tregs were first shown to secrete EVs in 2013 (Lesley Ann Smyth *et al.*, 2013; Yu *et al.*, 2013). (Lesley Ann Smyth *et al.*, 2013) showed the TCR-activation dependent release of EVs by Tregs. These Treg-EVs were then shown to express common T cell-associated surface proteins such as CD4, CD2, and MHC Class I. More interestingly, these Treg-EVs also expressed proteins such as CD25, CTLA-4 and CD73 which have been described to play a role in Treg-mediated suppression. The study went further to show the involvement of CD73 expressed on murine Treg-EVs in the suppression of Teffs in vitro, attributed to the conversion of Adenosine Monophosphate (AMP) to adenosine which has been shown to bind to Teffs and inhibit the secretion of IL-2 and IFN-γ. Building on this, Okoye *et al.*, (2014) showed that Tregs secreted the most EVs in comparison to other T cell subsets, further showing that the inhibition of EV production of EVs by Tregs drastically decreased the suppressive capacity of Tregs suggesting that this is an important mechanism involved in their function.

The study by Yu *et al.*, (2013) also highlighted that rat Treg-derived EVs were able to modulate transplant rejection in a rat kidney transplant model and prolong allograft survival. Tregs have been shown to secrete EVs that contain and transfer different molecules, such as microRNAs (miRNA), to DCs and T cells. Okoye et al., (2014) described the successful transfer of Treg EV associated miRNA Let7b leading to the suppression of pathogenic T helper 1 cells, whilst Tung et al., (2018) found that transfer of miRNAs 142-3p and miR150

present in murine Treg-EVs resulting in increased IL-10 production and decreased Interleukin 6 (IL- 6) production in DCs, following Lipopolysaccharide (LPS) stimulation. Furthermore, Treg-EVs can transport IL-35 to target cells, which both suppresses the target cell as well as converts the target cell to an IL-35 expressing cell, which in turn can suppress cells further in a contact dependent manner (Lema & Burlingham, 2019). Treg-EVs may mediate the delivery of apoptosis-inducing proteins such as granzymes and perforin (Gondek *et al.*, 2005) as well as inducible nitric oxide synthase (iNOS) as shown by Aiello *et al.*, (2017), who showed that after incubation with Treg-EVs apoptosis was induced in naïve T cells via its molecular cargo.

(Tung *et al.*, 2020) showed that activated human Tregs secrete EVs which are able to suppress Teffs in vitro as well as alter the cytokine profile to a more anti-inflammatory. Interestingly, the increase in IL-10 secretion by Teffs when incubated with Treg-EVs surpassed the secretion level of Teffs incubated with Tregs.

Therapeutic Potential of Regulatory T cell EVs

Adoptive transfer of Treg-EVs has been shown to lead to immune suppression in vivo. Liao, Lu and Dong, (2020) have shown that Treg-EVs induced proliferation and inhibited TNF-α mediated apoptosis of murine colonic epithelial cells through the delivery or miR-195-3p in vitro and alleviating induced inflammatory bowel disease (IBD) in a mouse model via the same mechanism. Specifically, in transplant settings, administration of Treg derived EVs have been shown to suppress rat kidney damage in a transplant model (Yu et al., 2013). Alloreactive T cell mediated damage in a humanised skin transplant model (Tung, et al., 2020) was also found to be reduced in the presence of these EVs. Humanised mice were used in a skin transplant model where a human skin xenograft was transplanted onto immune-deficient mice. 6 weeks post-transplantation, mice were infused with a human Teffs in conjunction with either Tregs or Treg-EVs. The Treg-EV treatment was shown to decrease the number of infiltrating CD45+ cells and Ki67+ keratinocytes, thus leading to protection of the allograft.

Targeting EVs

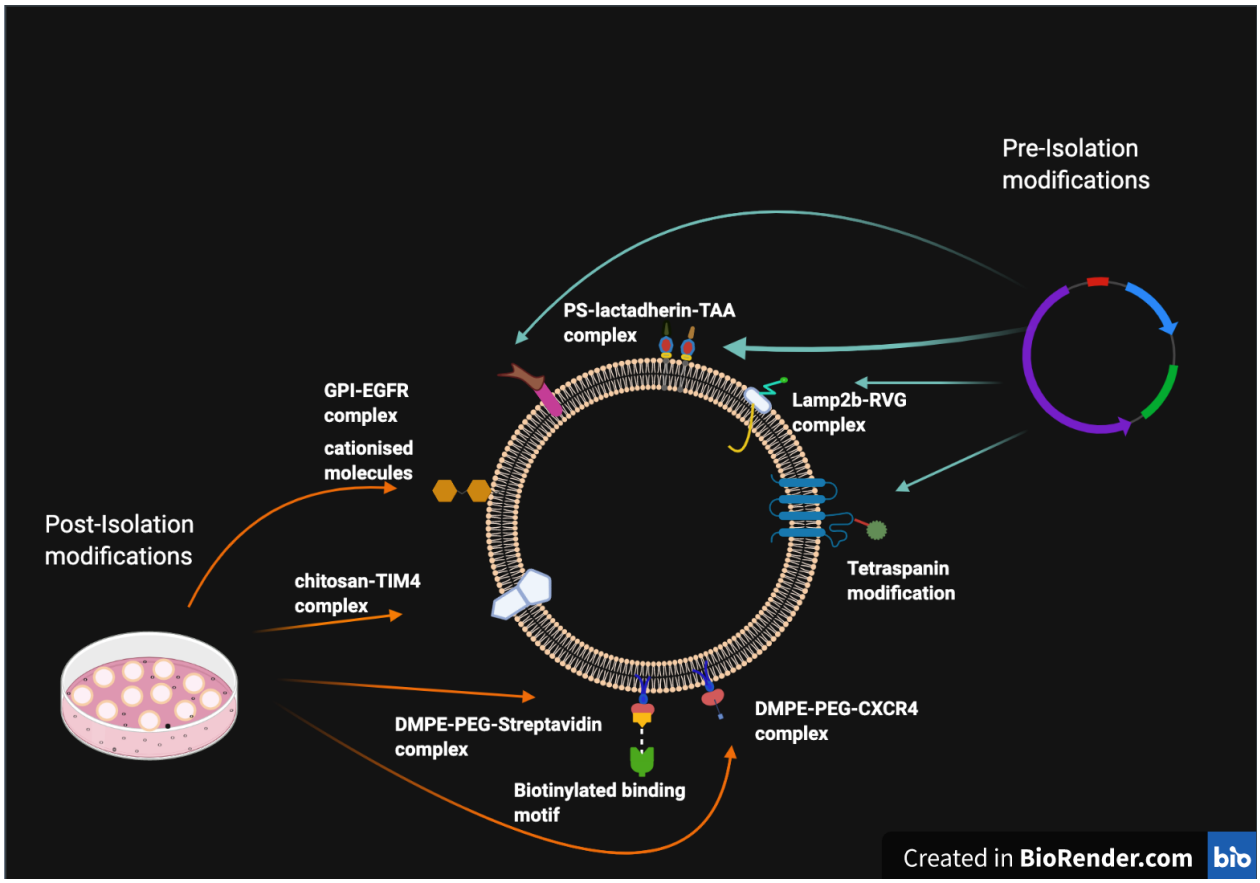

Figure 4*:* An illustration depicting potential pre-isolation and post-isolation targeting modification targets commonly found on EVs. Common pre-isolation targets are highlighted by the light blue arrows, while the orange arrows highlight common post-isolation targets.

One of the limitations of the therapeutic use of EVs is the limited understanding of the intrinsic specificity exhibited by EVs from different sources, as reviewed by Lara *et al.*, (2020). Targeting EVs has become common practice within the EV field as it increases the scope of their therapeutic use and may overcome this limitation.

The targeting of EVs is commonly achieved via a pre-isolation targeting method involving viral vector transfection of the parent cell to express specific proteins in EV membrane, thus allowing the isolation of EVs which express the intended protein on their surface (Figure 4). Knowledge of the cell surface molecules found on the target cell are essential for successful targeting of EVs using this method. This method of targeting EVs has been shown to successfully engineer targeted EVs by many studies (Delcayre *et al.*, 2005; Hartman *et al.*,

2011; Rountree *et al.*, 2011; Ohno *et al.*, 2013; Stickney *et al.*, 2016; Kooijmans *et al.*, 2018; Wang *et al.*, 2018). This often involves the transfection of cells to express a chimeric version of the C1C2 portion of lactadherin which has been shown to be incorporated in the membrane of EVs through association with PS (Andersen *et al.*, 2000). Clones containing the gene encoding the targeting motif are usually used to transfect the required parent cell in order to isolate EVs expressing the desired targeting motif.

Other studies have targeted EVs through the fusion of specific peptides to Lamp2b (Alvarez-Erviti *et al.*, 2011; Liu *et al.*, 2015; Wiklander *et al.*, 2015) and GPI (Sander A. A. Kooijmans *et al.*, 2016). Furthermore, (Stickney *et al.*, 2016) have shown the possibility to modify tetraspansins such as CD63 and CD81, commonly found in EVs, including Tregs EVs (Lesley Ann Smyth *et al.*, 2013; Tung *et al.*, 2020), which could potentially be used to express targeting motifs.

Although pre-isolation techniques have been shown to be successful in therapeutic treatment of certain diseases, the method still limits the potential of exosome-based therapy. Pre-isolation techniques require modifications of specific parent cells which prevents mass production of modified exosomes, therefore restricting potential therapeutic use. However, the use of post-isolation modification techniques (see Figure 5) presents an opportunity to mass produce engineered exosomes that are able to target any cell type with high specificity if the surface proteins of the cell are well understood.

There are also post-isolation techniques that are used to engineer EVs to target specific cells. The common targets of these modifications are: attachment to phospholipids such as PS (Hosseini *et al.*, 2016; Wang *et al.*, 2018), tetraspanins (Stickney *et al.*, 2016), GPI (Sander A. A. Kooijmans *et al.*, 2016) and Lamp-2b (Alvarez-Erviti *et al.*, 2011). Interestingly, Kooijmans *et al.*, (2018) showed that fusion proteins targeting Epidermal Growth Factor Receptor (EGFR) and lactadherin could bind to PS expressed on the surface of red blood cell (RBC) derived EVs via the C1C2 domain. This conjugation of PS with the C1C2 EGFR-targeting motif was shown to increase preferential uptake of targeted EVs to the EGFR expressing human epidermoid carcinoma cells over cells which did not express EGFR in vitro. Furthermore, this EGFR-targeting motif was shown to be able to bind to EVs derived from murine neuroblastoma cells, while maintaining similar in vitro uptake.

This suggests that this targeting motif could be used to target any PS-expressing EVs with similar outcomes as well as PS may constitute a promising EV surface protein anchor for the expression of targeting constructs used to increase the targeting specificity of EVs. The validation of PS expression on Treg-EVs would allow direct targeting similar to EVs derived from other parent cells, with the added suppressive functions displayed by Treg-EVs; inducing a regulatory mechanism which could potentially suppress B-cell mediated rejection.

EVs vs Tregs

Tregs used as therapeutics has long been stifled by the fact that the Tregs require ex-vivo expansion to be able to produce a therapeutic dose. As described by (Hippen *et al.*, 2011), there is a maximum number of three stimulations that Tregs can undergo without a drastic decrease in function. This has been a limiting factor for using Tregs therapeutically. EVs have been shown to have comparable, if not more efficient suppressive effects to Tregs(Okoye *et al.*, 2014), this is where using EVs instead of Tregs themselves presents an exciting opportunity for therapeutics. The stability of EVs in different environments in the periphery and the ability to manipulate EVs post-isolation further increases the adaptability of EVs as well as the potential of using EVs in a range of settings, including transplantation.

Aim and Objectives

The aim of the project was to create 'antigen (HLA-A2) specific' Treg-EVs via assessing the efficacy of post and pre isolation targeting regimes; targeting an anti- HLA-A2 antibody to Treg-derived EVs indirectly using phosphatidylserine (PS) and secondly using HLA-A2 specific CAR Tregs, respectively. This study will elucidate the possibility of developing targeted Treg-derived EVs to induce transplant specific tolerance and prolong allograft survival.

The objectives were:

- Assess whether Treg-EVs expressed PS and target EVs indirectly using this receptor
- Assess whether Treg-EVs isolated from Tregs expressed the HLA-A2 specific CAR on their surface
- Validate specificity of HLA-A2 specific Treg-derived EVs derived EVs to target HLA-A2 expressing B cells

Relevance of the research:

The long-term stability of infused Tregs remains unknown and is one of the concerns surrounding the use of these cells clinically. EVs isolated from these cells present a unique opportunity to produce the same effects, due to having functional similar to their parent cells (Fu *et al.*, 2019), in a much safer manner, as described by (Ha, Yang and Nadithe, 2016) and extensively reviewed by (Agarwal *et al.*, 2014).

The preclinical potential of Treg EV-based therapy has now been investigated and has shown promise in a human skin transplant model. However, there is a considerable gap in knowledge with respect to whether pre or post-isolation targeting of Treg-EVs to transplant tissues significantly increases specificity and improves outcome. The elucidation of a technique which will allow the generation of transplant antigen specific Treg EV-based immunotherapy could lead to targeting of specific immune cells involved in transplant rejection and help promote tolerance. This research aims to present proof-of-concept on targeting Treg-EVs for potential therapeutic use in the transplant setting, increasing specificity of the therapeutic product while bypassing the limitations of cellular therapy. If the overarching aim of the project is met this study will inform further research into actualising Treg-EVs as a potential plug-and-play therapeutic product for transplant patients.

Materials and Methods

Reagents and Solutions

All supplier information is described in Appendix 1.

The antibodies used to label samples for flow cytometry analysis, along with the companies from which they were purchased are described in Appendix 2.

Centrifugation

All centrifugation was performed at 1800rpm for 5 minutes at 4^{o}C using an Eppendorf 5920R centrifuge (ThermoFisher, Paisley, UK) unless stated otherwise.

Cell Lines

The human Tregs and CAR-Tregs were derived from established Treg and CAR-Treg cell lines, respectively, and were a kind gift from Dr Romano and Professor Lombardi, Immunoregulation Lab, Kings College London (KCL), UK. The Treg cell line was established for research into their therapeutic capacity and are characterised as $CD4^{+}CD25^{+}FoxP3^{+}$ T cells as described by (Scotta *et al.*, 2013; Safinia *et al.*, 2016; Romano *et al.*, 2018).

HLA-A2- (BM21) and HLA-A2+ (SPO) B cells were derived from established B cell lines and were a kind gift from Professor Lombardi, Immunoregulation Lab, KCL, UK. These cell lines are transformed lymphoblastoid B cell lines which have previously been used as a functional target for CAR expressing Tregs as described by (Mohseni *et al.*, 2021) and characteristically express HLA-A2 (SPO) or lack HLA-A2 expression (BM21).

Media

Treg lines were maintained in X-Vivo 15 (Lonza, Slough, UK) supplemented with 10% heat-inactivated, filtered Human Serum (HS) (Biowest, Nuaille, France) and 1% Penicillin-Streptomycin (ThermoFisher). For EV isolation these lines were cultured in EV free media consisted of X-Vivo 15 supplemented with heat-inactivated EV Free FCS (ThermoFisher).

B cells lines were grown in RPMI (Merck, Feltham, UK) supplemented with 10% heat-inactivated, filtered Foetal Calf Serum (FCS) (BioSera, East Sussex, UK), 1% Pen-Strep and 2mM of L-glutamine (ThermoFisher).

Treg and CAR-Treg Line Expansion

All Treg expansion reagents including X-Vivo 15, CD3/CD28 expansion beads (ThermoFisher), InterleukinL-2 (IL-2) (Proleukin, Novartis, UK) and Rapamycin (RAPA) (LC-Laboratories, MA, USA) were kindly gifted by Professor Giovanna Lombardi, Immunoregulation Labs (KCL).

Established human Treg and CAR expressing Treg cell lines were supplied as frozen pellets or as cells in suspension. For the former, aliquots were defrosted and plated at 1 x 10^6 cells/mL using X-Vivo 15 supplemented with 5% of human serum. The cells were aliquoted into a 24 well plate (ThermoFisher) and underwent expansion using anti-CD3/CD28 coated beads at a 1:1 cell: bead ratio. IL-2 and Rapamycin (RAPA) was added to the cells at 1000 U/mL and 100nM, respectively and subsequently every 2 days. On day 10, the Tregs were 'rested' for 2 days by the removal of the CD3/CD28 expansion beads and low-dose IL-2 (100 U/mL) before being re-stimulated for another 10 days or activated to produce Treg-EVs.

Cells that were re-stimulated further, were aspirated from the wells and the CD3/CD28 expansion beads were removed using a Dynamag-15 Magnetic Separator (ThermoFisher). The cells were then washed twice using X-Vivo 15, counted using a haemocytometer, with a 1:1 ratio with Trypan blue (ThermoFisher). These cells were then expanded further using anti-CD3/CD28 beads in the presence of IL-2 and RAPA, as above. In line with the current understanding of the effect of repeated stimulation has on the suppressive capacity of ex vivo expanded Tregs as described by Hippen *et al.*, (2011), the Treg cell lines were stimulated a maximum of three times.

Expanded Treg Phenotyping

Expanded Treg cells were phenotypically analysed using flow cytometry. The antibodies used, along with the companies from which they were purchased are described in Appendix 2. 1x10^5 cells in 100uls FACS buffer (PBS + 2% FCS and 0.1% EDTA) were added into separate wells of a 96 U-bottom well plate and 1µL of each of the following antibodies: anti-CD4-PE, anti-CD25-PE and anti-CD127-FITC added for 30 minutes at 4ºC. Subsequently,

the samples were washed twice with FACS buffer, by centrifugation before being resuspended in 400µL of Fluorescence-activated Cell Sorting (FACS) buffer. Unstained Tregs were used as a control to set the gating strategy used for each marker.
Green Fluorescence Protein (GFP) expression on CAR-Treg cells was also investigated to confirm the expression of the CAR motif.
Sample analysis was performed using an Accuri C6 or a BD FACS Celesta flow cytometer (BD Biosciences, Franklin Lakes, NJ, USA) and the data collected was further analysed using Flow Jo (Tree Star, OR, USA).

EV Isolation

After the 2-day rest period where the beads were removed and cells were incubated with low-dose IL-2. The Tregs were harvested from the culture medium, washed with room temperature Roswell Park Memorial Institute Medium (RPMI) and counted using Trypan Blue. Tregs were then labelled with Carboxyfluorescein succinimidyl ester (CFSE) (ThermoFisher) according to manufacturer instructions for further downstream applications. To achieve this, 5mM CFSE stock was diluted to 0.5µM using pre-warmed PBS. 1mL of 0.5µM CFSE per $1x10^7$ cells was then used to stain the cells. The cells were incubated at 37ºC for 15 minutes before being washed in 5x the volume of FCS-containing media was used to wash the cells twice. The CFSE-labelled cells were then resuspended at $3x10^6$ cells/mL in Exo-Free Media FCS (ThermoFisher) for subsequent activation. Small aliquots of unstained Tregs and the CFSE-labelled Tregs were utilised to confirm successful CFSE-labelling using flow cytometry.

To activate the Tregs, 24-well plates were coated with 5µg/mL and 10µg/mL of anti-CD3 (ThermoFisher) and anti-CD28 antibodies (a kind gift from Dr Tung, KCL, UK) in PBS (ThermoFisher), respectively, at 37ºC for at least 2 hours. After the incubation the antibody-coated 24-well plate was washed with PBS to remove unbound antibody and the Tregs were then seeded at 3 $x10^6$ cells in 1mL per well of EV free media and incubated for 24 hours at 37ºC.

To isolate EVs, the culture supernatants were harvested from the culture plates and centrifuged to pellet cells and cellular debris, which were discarded. The supernatant was aspirated and filtered using a 0.22µm filter (Milteniyi, Surrey, UK) to remove any large

vesicles and other cell fragments and contaminants above the size of the 0.22µm threshold. Following this, 1mL of Exoquick (System Biosciences, Palo Alto, CA, USA) was added for every 5mL of supernatant harvested and gently mixed by inversion of the tube. At the same time, Exoquick was added to a similar volume of EV free media and will serve as a 'Media-EV pellet' control. The Exoquick/supernatant mixture was then incubated at 4ºC overnight and the following day, the solution was centrifuged at 1500 x g for 30 minutes. The supernatant was discarded, leaving ~500µL which was centrifuged for a further 5 minutes to maximise the amount of EV harvested. The remaining supernatant was carefully aspirated, and the EV rich pellet was resuspended in the necessary media, according to the requirements for the downstream applications.

In some experiments, CD81-Dynabeads (ThermoFisher) were used according to the manufacturer instructions. Briefly, the CD81 beads stock ($4.8x10^6$ beads/mL) was vortexed to resuspend the beads and diluted 1:4 in isolation buffer (PBS supplemented with 0.1% BSA). 1mL of Isolation Buffer was added to the Dynabeads to wash the beads. The solution beads were then isolated from the solution using a Dynamag Magnetic Separator (ThermoFisher) for 2 minutes. The buffer was aspirated and discarded. The beads were then resuspended in 90µL of Isolation buffer. 10µL of isolated CAR-EVs was then added to the solution and incubated overnight at 4ºC. 1mL of isolation buffer was then added to the tube and the magnetic separator magnet was used for 2 minutes to re-isolate the beads The tube was removed from the magnet and the beads were resuspended in 0.5mL of isolation buffer and then re-isolated by magnetic separation. Finally, the EVs were resuspended in 200µL of FACS buffer.

CD81 Treg-EV Validation

Post isolation, Treg-EVs were validated using CD81 (EXOELISA-CD81, System Biosciences) according to the commercial protocol. Briefly, EVs isolated from $1\text{-}10x10^6$ Tregs were diluted in coating buffer up to 120 µL. The protein standard was also prepared according to the commercial protocol, using a serial dilution of the 1/1000 diluted protein standard stock in coating buffer. 50 µL of each donor sample and each standard was added to the Enzyme-linked Immunosorbent Assay (ELISA) strip wells in duplicate. The wells were incubated at 37ºC for 1 hour with shaking, before being washed with wash buffer 3 times for 5 minutes with 100µL of wash buffer. The CD63 or CD81 primary antibody was diluted

1/2000 with blocking buffer and 50µL was added to each well. The plate was incubated for 1 hour with shaking at room temperature before being washed 3 times for 5 minutes with 100µL of wash buffer. The Horseradish peroxidase (HRP)-conjugated secondary antibody was diluted 1/5000 with blocking buffer and 50µL was added to each well. The plate was incubated for 1 hour, with agitation, at room temperature before being washed 3 times for 5 minutes with 100µL of wash buffer. 50 µL of room temperature, super-sensitive 3,3′,5,5′-Tetramethylbenzidine (TMB) was added to each well and the plate was incubated at room temperature with shaking for 5-15 minutes, depending on the speed of the colour change. 50µL of stop solution (0.16M sulfuric acid) was added and the plate was read at 450nm immediately using a microplate reader (Biotek Synergy HTX multimode plate reader). A media EV pellet was resuspended in exosome binding buffer to be used as a negative control.

Phosphatidylserine (PS) ELISA

The expression of PS on the Treg-EVs was assessed using a PS-detection ELISA, according to the commercial protocol (Alpha laboratories, Eastleigh, UK). Briefly, the EVs isolated from 1-2x10^6 Tregs from each donor line were diluted in reaction buffer and added in duplicates to single wells of the Tim4-coated PS-capture ELISA microplate and incubated with shaking at room temperature for 2 hours. The wells were washed with 350µL of wash buffer 3 times before addition of an anti-CD63 primary antibody (1/100 dilution) for a further hour at room temperature with shaking. A 1/100 dilution of the HRP-conjugated Streptavidin secondary antibody was added after washing wells 3 times with 350µls of wash buffer. The plate was incubated at room temperature for another 2 hours, with shaking. Lastly, wells were washed, as described before, and 100uls of TMB solution was added for 30 minutes at room temperature before the stop solution (0.16M sulfuric acid) was added. Plates were read at 600nm using a micro-plate reader (Biotek Synergy HTX multimode plate reader)). A media EV pellet was resuspended in reaction buffer and used as a negative control.

Micro-BCA Assay

The protein content of isolated Treg-EV samples was analysed using a Pierce micro-BCA Protein Assay Kit (Thermofisher, UK) according to the standard protocol. Briefly, EVs isolated from 1-2x10^6 and control media pellet were diluted to 300µL with working reagent. The EV samples were not lysed with lysing buffer. This is because the interest was in evaluating the level of surface proteins found on the EVs to anchor the targeting motif. The

amount of internal protein of the EV samples were irrelevant to the main interest of this study. The Bovine Serum Albumin (BSA) standards were prepared according to the standard protocol. 150µL of each protein standard, the control sample and the EVs from each donor were added to duplicate wells. 150µL of working reagent was then added to each well and the plate was mixed using a microplate shaker for 30 seconds. The plate was sealed and incubated at 37ºC for 2 hours. The absorbance of the wells was measured at 562nm using a microplate reader. The standard curve produced using the standards was used to calculate the unknown protein concentration of the EV samples.

X-Stamp Treg-EV decoration

10 µL of X-Stamp Pro-Streptavidin (SystemBioscience, Colne, UK) was incubated with every 300µg of protein in each EV sample for 1 hour at room temperature in a total volume of 300µL, topped up with Exo-Free Media. The EVs were re-isolated post-decoration using Exoquick. Briefly, 100mL of ExoQuick was added to the 'decorated' EVs and they were incubated overnight at 4ºC. The EVs sample was then centrifuged at 14000rpm in a microfuge (make model) and the EV pellets were resuspended in ExoFree Media. The re-isolated 'decorated' EVs were then incubated with a biotinylated 5µL anti-HLA-A2 (Miltenyi, Surrey, UK) for an hour at room temperature.

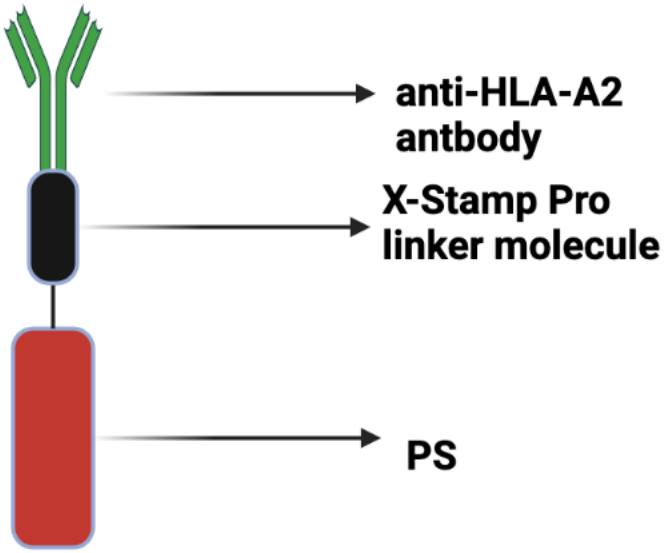

Figure 5: An illustrative diagram to highlight the structure of the PS-anchored HLA-A2 targeting motif.

Targeting of Xstamp Pro 'decorated' Treg-EV to B cells.

HLA-A2+ B cells and HLA-A2- B cell lines (a kind gift from Adeel Saleem, KCL, UK) were cultured and expanded in B cell expansion media at a concentration of $0.3x10^6$ cells/mL for 7 days in T25 flasks. Cell counts were checked every two days and sufficient fresh media was added to culture to keep the cells at the correct concentration. At the end of culture, the cells were harvested, counted and resuspended at the appropriate concentration for the co-culture experiments. HLA-A2 expression was validated using flow cytometry. Briefly, $1x10^5$ cells aliquoted in 100µL of FACS buffer were stained with 1µL of anti-HLA-A2 antibody-PE with HLA-A2- Tregs used as a negative control. The stained cells were incubated at 4ºC for 20 minutes. Following incubation, the cells were washed twice with FACS buffer and resuspended with 200µL of FACS buffer. Unstained B cells were used to set the initial gating strategy for analysis.

CFSE-labelled 'decorated' and control 'naïve' Treg-EVs were each co-cultured for 24 hours at 37ºC with HLA-$A2^+$ B cells at a ratio of 100:1 (EVs isolated from $1x10^6$ Tregs were co-culture with $1x10^4$ B cells). Following this incubation, the B cells were analysed via flow cytometry for expression of CFSE fluorescence. Treg-EVs isolated from each donor Treg line were targeted once.

Validation of CAR expression of CAR-Treg derived EVs

EVs derived from CAR-Tregs were incubated with anti-CD81 antibody coated beads overnight at 4ºC with end-to-end mixing, as described previously. Following incubation, the beads were washed to remove unbound EVs and stained with anti-CD25 antibody (PE) as well as anti-c-Myc antibody (PE-CF594). The stained beads were then washed twice to remove any unbound antibody, as previously described, and analysed using the BD Celesta and Flowjo software analysis.

Co-culture of CAR-Treg-EVs with B cells

CFSE-labelled CAR-Treg-EVs were co-cultured for 24 hours at 37ºC with HLA-A2^{+} B cells and HLA-A2^{-} B cells at a ratio of 100:1, see above. Following this incubation, the B cells were analysed via flow cytometry for CFSE fluorescence. Naïve EVs were used as controls. Due to the number of Tregs expanded, EVs isolated from each donor were only incubated with target cells once.

Statistical analysis

Statistical analysis was employed to assess the statistical significance of the data reported in this project. Using GraphPad Prism 9.2 software, non-parametric two-tailed T-tests, one-way Analaysis of Variance (ANOVA), and two-way ANOVA, with multiple comparison of means, was used to analyse the significant differences between groups of data. In this report, * denotes a p value of <0.05, ** denotes a p value of <0.01, **** denotes a p value of <0.0001, while ns is used to denote no statistical significance.

Results

Characterisation of $CD4^+CD25^+CD127^{lo}$ Expanded Tregs

From previous studies Treg-derived EVs have been shown to be reliably isolated from at least 1-5x10^6 Tregs (Tung, 2020). To set up the fundamental EVs experiments for this study, established Treg lines had to be expanded to achieve this number of cells. In order to validate the successful expansion of established Treg cell lines, and lend credibility to the ability to isolate Treg-derived EVs, the purity of the cell cultures and the phenotypical nature of the expanded Tregs was assessed against characteristic markers described by Ballke *et al.*, (2016) & Issa *et al.*, (2019), using flow cytometry. To assess expression of CD4, CD25 and CD127 on the Treg cell lines, the cells were rested for 48 hours after the expansion protocol. Cells were stained with anti-CD4 PE, anti-CD25 PE and anti-CD127-FITC antibodies and subsequently analysed using flow cytometry. The results of one Treg line is depicted in Figure 6 A and B. The knowledge of typical lymphocyte forward (FSC) and side scatter (SSC) distribution was used to establish the lymphocyte population and negate any cell debris and dead cells from further analyses as shown in Figure 6A. The mean population of lymphocytes post-expansion was found to 47.3% (check FSC vs SSC plots for each donor and calculate mean). Using unstained cells (Figure 6B) to set up a negative gating strategy, the lymphocyte population was then used to analyse CD4 expression, which can be used to confirm the presence of T cells in a sample. The results showed that there was a 91.8% T cell purity in the sample as shown in Figure 6C(i). The T cells were then assessed for the expression of Treg-associated proteins such as CD25 which is closely related to the regulatory function of Tregs (Zhao, Liao and Kang, 2017) and thus is expected to be highly expressed. The results showed that 62.0% of the T cell population were $CD25^+$ as shown in Figure 6C(ii). CD127lo Tregs are a specific subtype of Tregs which have been shown to be highly suppressive (Sharma *et al.*, 2015; Ius *et al.*, 2019). The results shown very little CD127 expression, 0.41% of the sample expressed CD127 beyond what is assumed to be background, set using the negative control unstained cells, and of those that did the expression was at low levels as depicted in Figure 6C(iii). Figure 6D shows pooled data from the characterisation of several independently expanded Treg cultures. Similarly, to what we observed above, the expression of CD4 and CD25 on each Treg expansion were consistently significantly higher than background fluorescence of unstained cells. The expression of

CD127 was also determined to be significant showing that there is a small population of our Tregs which express low levels of CD127.

In conclusion, as expected and in line with literature (Tung, 2020) the expansion protocol used led to Tregs which expressed Treg-associated proteins.

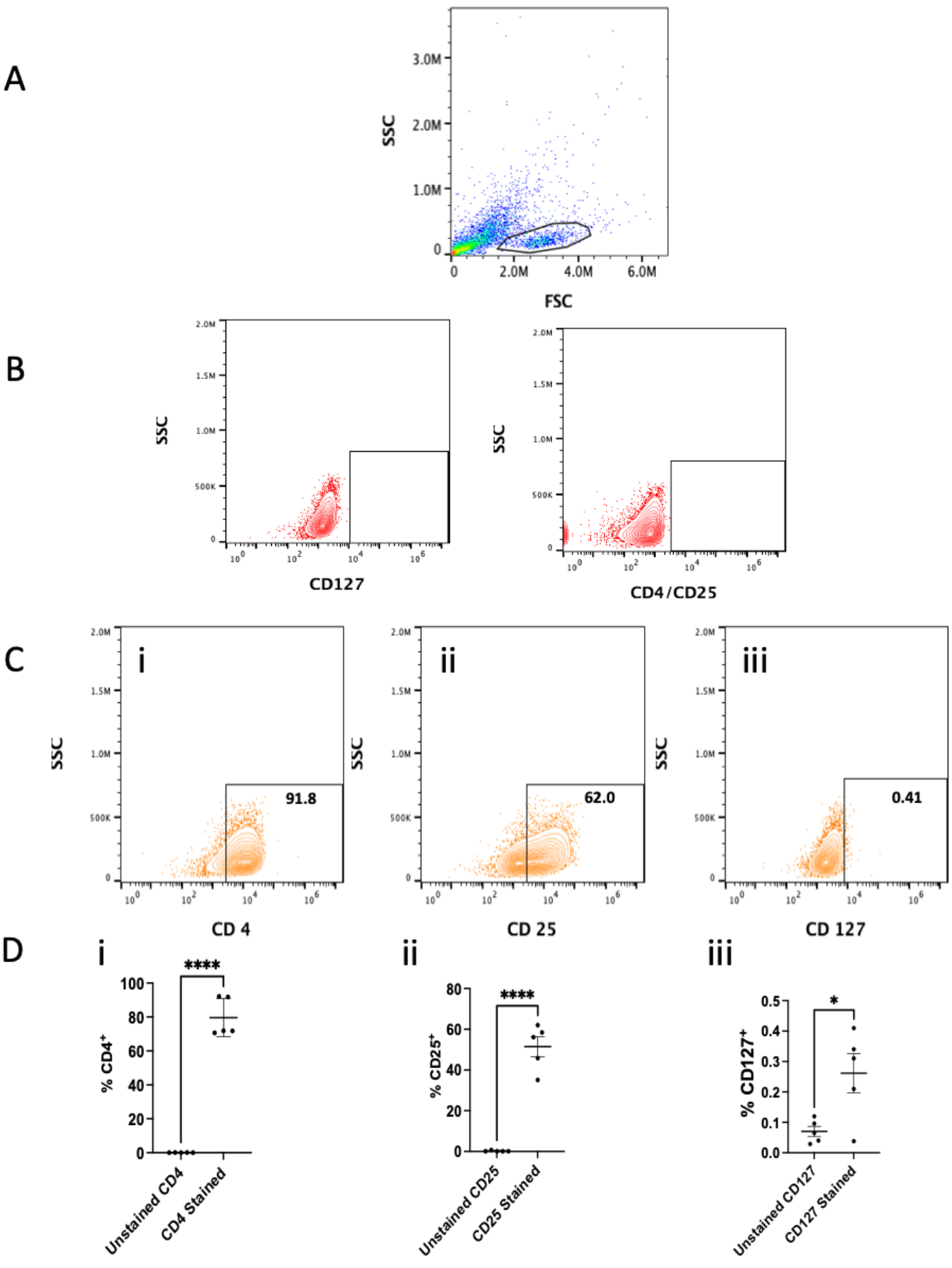
A
SSC
FSC
B
CD127
CD4/CD25
C
i
ii
iii
91.8
62.0
0.41
CD 4
CD 25
CD 127
D
% CD4+
% CD25+
% CD127+
Unstained CD4
CD4 Stained
Unstained CD25
CD25 Stained
Unstained CD127
CD127 Stained

Figure 6: Confirmation of expression of Treg cell markers. Expanded Treg cell lines were analysed via flow cytometry to assess the expression of surface proteins commonly used to characterise Tregs. A. Dot plot depicting the gating strategy employed to analyse the lymphocyte population in the sample using the known size and granularity of T cells, n=1. B. Contour plot depicting gating strategy for both PE and FITC fluorescence using unstained B cells, n=1. C. Contour plots depicting CD4 (i), Cd25 (ii) and CD127 (iii) expression of stained B cells, (n=1). Comparative statistical analysis was carried out using a t-test to assess the significance of CD4, CD25 and CD127 expression on Tregs vs the unstained cells, as shown in Figures 4D(i), 4c(ii) and 4c(iii), respectively. * Denotes a P-value of <0.05 while **** denotes a P value of <0.0001.

Validating CD81 expression of Treg-EVs using an anti-CD81 ELISA.

(Tung *et al.*, 2020) have characterised Treg-EVs according to the requirements aid out by the International Society of Extracellular Vesicles (ISEV) (Théry *et al.*, 2018). They published that these vesicles expressed CD63, CD81, CD25, CD39 and had low-levels of CD4 and CTLA-4, but lacked FasL and CD73 expression. CD81 has been shown to be a reliable, commonly used EV marker and was shown previously to be expressed by Treg EVs as mentioned by (Tung *et al.*, 2020). In order to confirm CD81 expressing EVs could be isolated reliably from expanded Tregs, we activated rested Tregs using a combination of plate bound anti-CD3 and anti-CD28 antibodies, for 24 hours, in EV free media. EVs were then isolated from the aspirated media supernatant using the ExoQuick method, as previously described(Tung *et al.*, 2020). To confirm the presence of EVs in our samples, CD81 expression was assessed using a CD81 ELISA. Using a standard curve, as shown in Figure 7a(i), allowed the calculation of the number of EVs in our sample that expressed CD81. Statistical analysis confirmed that CD81 expressing EVs were isolated from activated Tregs as compared with media pellet, which we did not expect to contain any EVs, Figure 7a(ii). The data also showed that there was variability in the amount of CD81 expressing EVs isolated from the different Treg cell lines used, again confirming previous data (Tung et al).

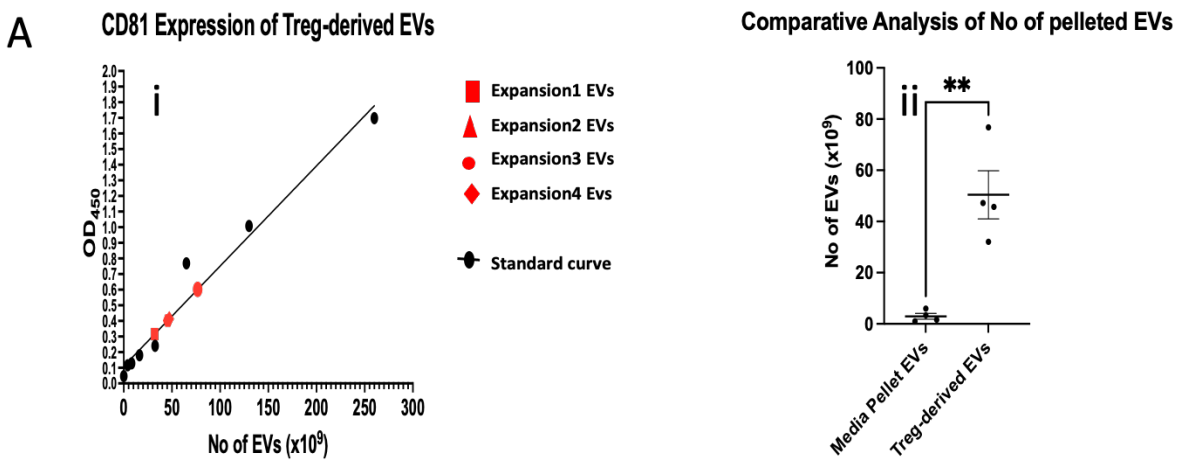

Figure 7: Expression of CD81 on Treg-derived EVs. A(i). A graph depicting the standard curve used to calculate the number of CD81+ EVs in the samples. Each red dot represents the average OD value from a technical duplicate for 4 independently isolated EV samples from 4 independent Treg expansions. A(ii) a graph depicting the mean (+/- SD) number of CD81+ EVs isolated from the Treg-derived EV samples, calculated using the CD81 ELISA. Media Pellet EVs represent the negative control group. Each dot represents the average OD values from duplicate samples from 4 independently isolated EV samples. ** Denotes a significant p-value of <0.01 calculated using a t-test.

Confirmation of Phosphatidylserine (PS) expression on Treg-EVs

In accordance with one of our principal aims, we investigated the expression of PS on Treg-EVs, which has not been shown to our knowledge. This investigation was carried out in an effort to elucidate the potential of using a post-isolation modification method to target Treg-EVs to HLA-A2 expressing cells using a commercially available linker molecule, X-Stamp Pro. This technique allows the targeting of any antigen using a biotinylated antibody raised against it. PS is a key protein that the X-Stamp Pro molecule binds to, serving as the base of the targeting platform. Thus, isolated Treg-EV samples were analysed for the expression of PS. To confirm the expression of PS, Treg-EVs were analysed using a PS-capture EV ELISA according to the manufacturer instructions. The result from this experiment showed that all Treg EVs isolated from different donor Treg lines expressed PS, in comparison to the control sample of media pellet EVs. However, as with CD81, PS expression variated between donors (Figure 8 A and B).

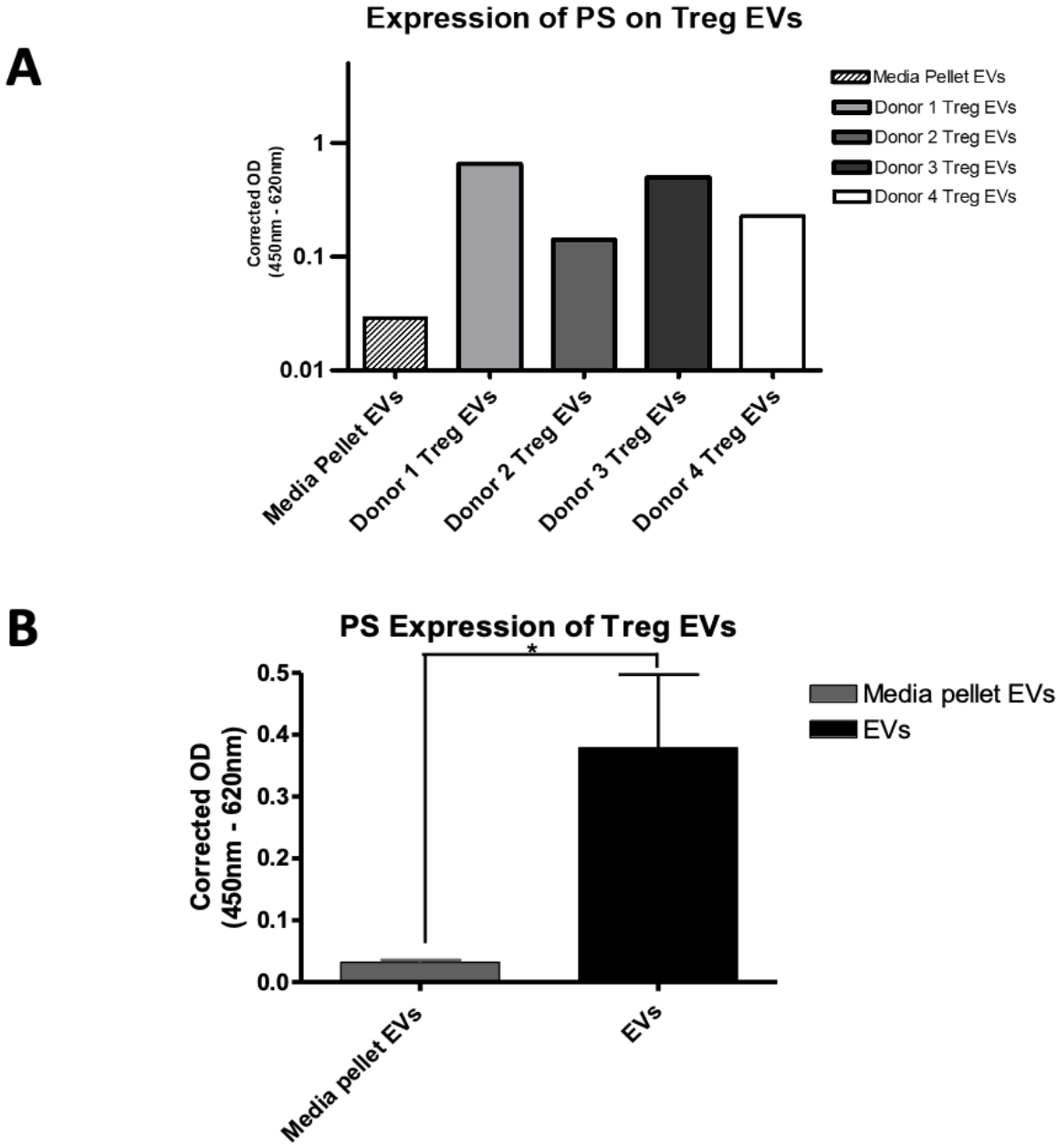

Figure 8: Expression of Phosphatidyl serine on Treg-derived EVs. A. Bar chart depicting the average corrected optical density of the sample, calculated by subtracting the optical density at 620 nm from the optical density at 450 nm from technical duplicate samples for PS expression as assessed using a PS specific ELISA. Media Pellet EVs, represents a negative control. Each bar represents one donor, tested in duplicate. Figure 8b is a bar chart depicting the pooled PS expression of Treg-EVs (n=4 donors) compared to media pellet EVs. Mean +/- 1SD is shown * Denotes a p-value of <0.05 calculated using a t-test.

CFSE-labelling of Tregs

Having shown PS expression, post-isolation decoration of the human Treg-EVs using the X-Stamp Pro reagent was possible. In previously published work, CFSE-labelling of the parent cell has been shown to be a reliable method used to assess EV acquisition (Tung, 2020). To produce CFSE-labelled EVs, for validation of acquisition of post-isolation modified EVs, rested Tregs were labelled with CFSE, as described in the methods section, before being activated for EV release, as above.

Prior to activation of the Tregs, CFSE expression was confirmed to ensure that the staining was successful. The FSC and SSC gating strategy of the cells is shown in Figure 9a. As shown, 48.5% of the sample were the cells of interest based on their size and granularity. Using unstained Tregs (CFSE), a gate was set up as shown in Figure 9b(i). The CFSE-stained cells were then analysed and confirmed that 100% of the labelled Tregs were $CFSE^+$, suggesting that the staining step was successful. Further analysis of several independent CFSE staining procedures, shown in Figure 9c, confirmed that the protocol used reliably stained Tregs with high expression of CFSE. Statistical analysis confirmed, with over 99.9% confidence, that this staining procedure resulted in $CFSE^+$ cells in comparison to unstained cells, suggesting that EVs isolated from these cells would express CFSE as previously observed (Tung, 2020). Given this finding $CFSE^+$ EV acquisition following post isolation modification was assessed.

A

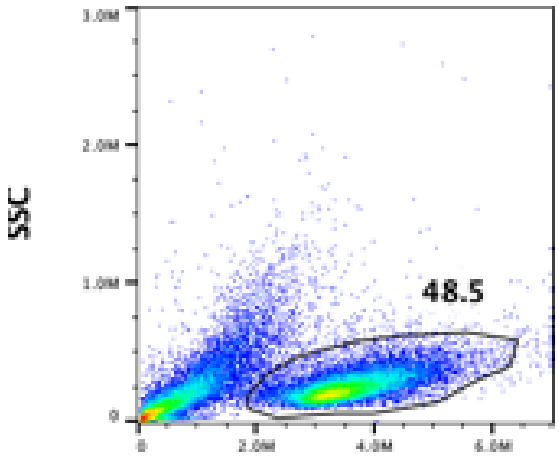
SSC
48.5
FSC

B

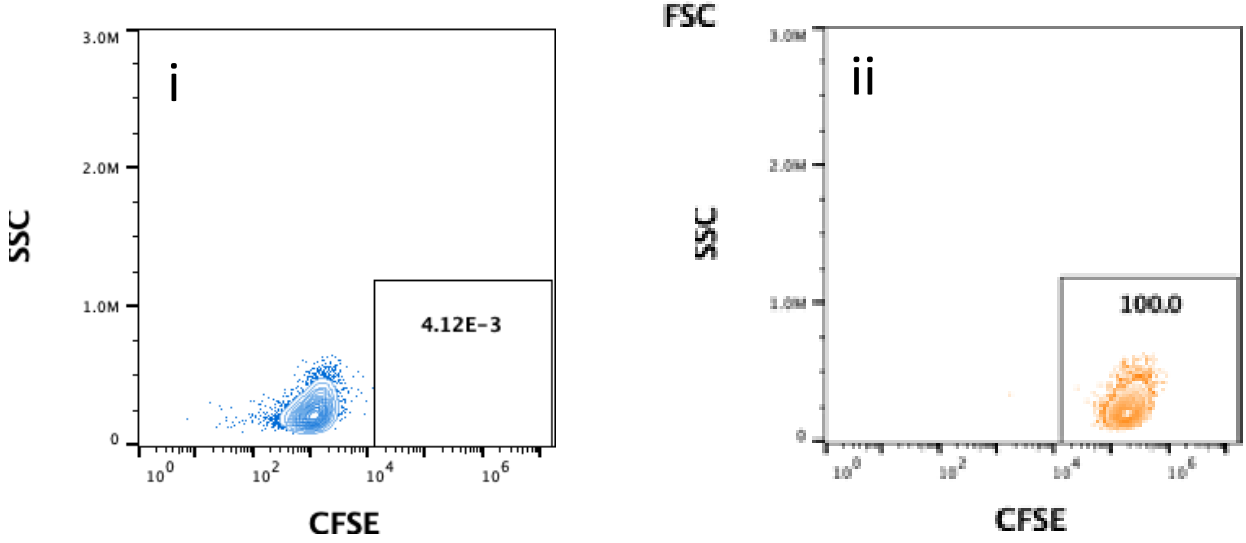
i
ii
SSC
4.12E-3
100.0
CFSE
CFSE

C

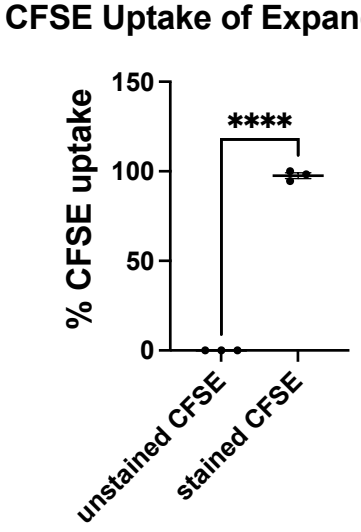
CFSE Uptake of Expanded Tregs
% CFSE uptake
****
unstained CFSE
stained CFSE

Figure 9: Confirmation of expression of CFSE on expanded Treg lines. Figure 9a depicts a FSC vs SSC dot plot used to gate on the lymphocyte population based on the expected size and granularity. Figure 9b(i) depicts a CFSE vs SSC contour plot of unstained control Treg sample to set up gating strategy for CFSE fluorescence which accounts for background fluorescence of Tregs in this channel. Figure 9b(ii) depicts a contour plot of CFSE fluorescence of the CFSE-stained Treg sample. Figure 9C is a graph depicting statistical analysis carried out to compare significant expression of CFSE on several independent CFSE-stained Treg cultures in comparison to the unstained Treg samples. **** Denotes a P value <0.0001 as calculated using a T-test.

Confirmation of HLA-A2 expression on expanded B cells lines

The aim of the project was to target Treg EVs to cells expressing HLA-A2. To this end, two B cell lines, one expressing HLA-A2 and a control line not expressing this molecule were acquired. To confirm HLA-A2 expression on these B cell lines we stained both with a PE-conjugated anti-HLA-A2 antibody and assessed the cells via flow cytometry. The B cell population for each sample was gated using an FSC vs SSC plot as shown in Figure 10a(i) and 8b(i). Unstained HLA-A2 B cells were used to set up the gating for HLA-A2 expression following staining. As expected, the HLA-A2 negative B cell line lacked expression of HLA-A2, with a small overall increase in Mean Fluorescence Index (MFI) in comparison to the control seen following antibody staining (Figure 10a(ii)). However, as expected, the HLA-A2+ B cells line showed a 7-fold increase in MFI (Figure 10b(ii)), over unstained cells, however only 60% of the B cells in the sample expressed HLA-A2.

Having confirmed that one of our B cell lines expressed HLA-A2, the target protein of the EV targeting strategy, and the other B cell line lacked the expression of this protein, we had the appropriate target cell as well as the appropriate control cell line to investigate the potential of the targeting procedure to increase the target specificity of Treg-EVs.

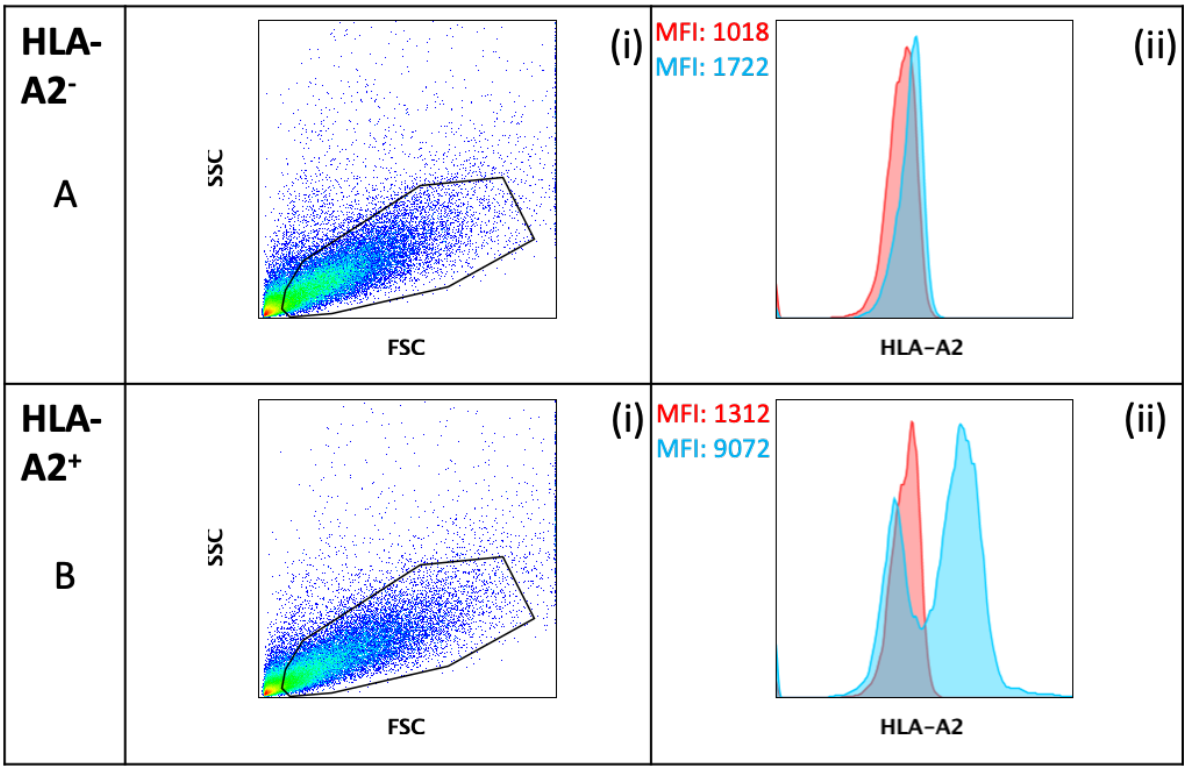

Figure 10: Confirmation of expression of HLA-A2 on expanded B cell lines. A(i). Psuedocolour plot depicting a FSC vs SSC dot plot used to gate on the B cell population of the expanded HLA-A2$^-$ B cells. The black polygon gate shows the population of cells in the sample expected to be the HLA-A2$^-$B cells. A(ii). Normalised histogram overlay plot depicting the HLA-A2 expression of the control, shown in red and the HLA-A2 stained HLA-A2- B cells, shown in blue, both of which are gated on the B cell gate depicted in Figure 10a(i). B(i). Psuedocolour plot depicting a FSC vs SSC dot plot used to gate on the B cell population of the expanded HLA-A2$^+$ B cells. The black polygon gate shows the population of cells in the sample expected to be the HLA-A2$^+$B cells. B(ii). Normalised histogram overlay plot depicting the HLA-A2 expression of the control, shown in red and the HLA-A2 stained HLA-A2$^+$ B cells, shown in blue, both of which are gated on the expected B cell gate depicted in Figure 10b(i).

Treg-EV Acquisition by B cells is mediated via PS.

Treg-EVs have been shown to be acquired by a variety of cells such as DCs (Tung *et al.*, 2018) and T cells (Yu *et al.*, 2013; Aiello *et al.*, 2017; Tung *et al.*, 2020). Previous work has also shown that B cells have the ability to acquire EVs, although from murine bone marrow-derived DCs (BM-DCs) (Becker *et al.*, 2021). This developed the interest to elucidate the potential of Treg-EVs to be acquired by HLA-A2 expressing B cells. Thus, we investigated the acquisition of naïve and targeted EVs by B cells. Briefly, PS expressed on the surface of

Treg-EVs were decorated with X-Stamp Pro, a linker molecule, which was subsequently directly conjugated with an anti-HLA-A2 antibody in order to target Treg-EVs to HLA-A2 expressing cells. Firstly, HLA-A2- B cells were co-cultured with naïve Treg-EVs at a ratio of 1:100, respectively, for 24 hours. Using non-EV treated B cells (control), a gating strategy was set to negate any background CFSE fluorescence, allowing us to assess the level of CFSE uptake via Treg-EVs in our experimental samples. The results showed an increase in the expression of CFSE on recipient cells, with a 2.75-fold increase in overall CFSE MFI expression as compared to control B cells (Figure 11b), suggesting that B cells were able to naturally acquire Treg-EVs without the need for targeting. This consistent increase in CFSE expression, and therefore Treg-EV acquisition, was found to be statistically significant when compared to the control group of unstained B cells incubated alone (Figure 11c). This control experiment of our targeting system was important to validate the ability for B cells to acquire human Treg-EVs.

Next, an experiment was set up to confirm that targeting Treg-EVs to HLA-A2 did not increase their acquisition by B cells not expressing the target, but rather be comparable to acquisition of naïve Treg-EVs. The experiment involved the incubation of targeted Treg-EVs with HLA-A2- B cells at a ratio of 100:1, respectively, for 24 hours. Briefly, PS expressed on the surface of Treg-EVs were decorated with X-Stamp Pro, a linker molecule, which was subsequently directly conjugated with an anti-HLA-A2 antibody in order to target Treg-EVs to HLA-A2 expressing cells. The results show an increase in CFSE expression on B cells (Figure 11c). Interestingly, the increase was accompanied with a fold increase in MFI of only 1.90 which is lower in comparison to incubation with naïve EVs, representing a relative decrease of 30.8%. The difference between the acquisition of naïve Treg-EVs and targeted Treg-EVs was found to be statistically significant. These unexpected results suggest that PS may be involved in the acquisition of human Treg EVs by B cells and potentially other cells in vitro.

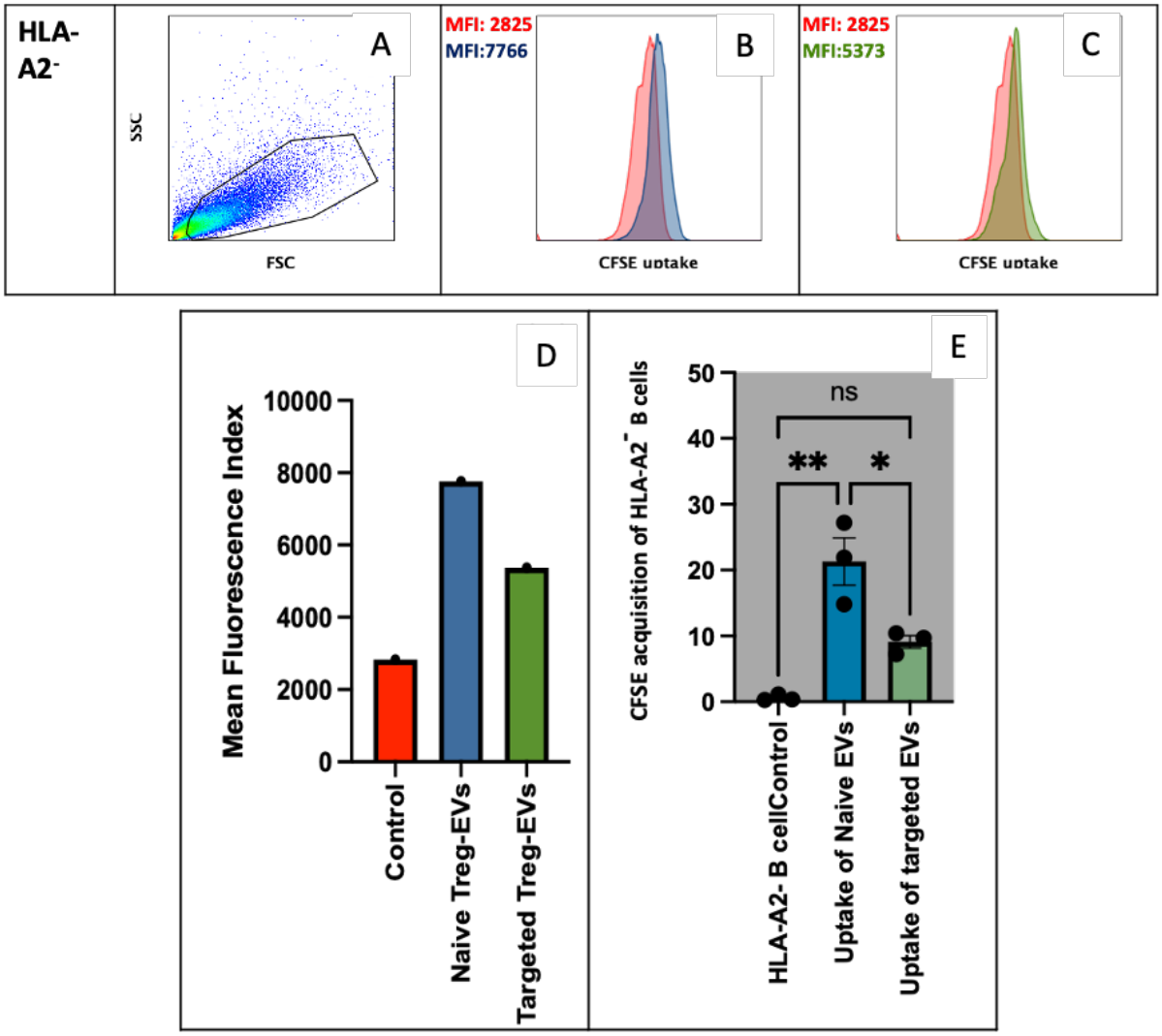

Figure 11: Acquisition of naïve and targeted Treg-EVs by HLA-A2- B cells. The B cells in each sample, except the control were incubated at a ratio of 1 B cell with EVs isolated from 100 Tregs. A. FSC vs SSC pseudocolour plot used to gate on the expected B cell population of the expanded HLA-A2- B cells. B. A normalised histogram overlay plot depicting CFSE expression of the B cells only control, shown in red and the HLA-A2+ B cells incubated with naïve EVs shown in dark blue, both gated on the cells shown in Figure 11a. C. A normalised histogram overlay plot depicting CFSE expression of the B cells only control, shown in red and the B cells incubated with targeted Teg-EVs, shown in green, both gated on the cells shown in Figure 11a. D. Bar chart depicting the MFI between control group, Naïve Treg-EV treated group and targeted Treg-EV group, n=1 experiment. E. Bar chart depicting the mean % of CFSE+ B cells post-incubation with CFSE-labelled Treg-EVs. Each dot represents the mean +/- SD CFSE expression of B cells analysed in 3 independent experiments, using 3 different donors. Data in Figure 11a-9c represents one experiment with one donor only whilst data in 9d and 9e are from 3 lines. MFI = mean fluorescence index. ns denotes no significance between groups, * denotes a p value of <0.05 and ** denotes a p value of <0.01 calculated using a two-way ANOVA.

Post Isolation PS-mediated targeting did not create antigen specific Treg-EVs

Next, we investigated whether targeting Treg-EVs increased acquisition and overcame the inhibition observed above when the target antigen HLA-A2 was present on the B cells. To this end, we decorated isolated Treg-EVs with a X-Stamp Pro Streptavidin-Biotin binding moiety according to the manufacturer instructions. Then, X-Stamp Pro decorated Treg-EVs were incubated with biotinylated anti-HLA-A2 antibody, of the same clone used to confirm HLA expression on the B cells. This antibody was used to increase targeting specificity of Treg-EVs to cell lines expressing HLA-A2. To assess acquisition, CFSE-labelled targeted Treg-EVs were incubated with B cells expressing the target protein, HLA-A2, at a ratio of 100:1 for 24 hours. Similarly, as a control, we also incubated CFSE-labelled naïve Treg-EVs with HLA-A2+ B cells.

The B cells were then analysed for CFSE expression using flow cytometry, as the CFSE expression of these unstained B cells post-incubation with CFSE-labelled Treg-EVs can be used to indirectly quantify Treg-EV acquisition as the two parameters are directly correlated. Our results show an increase in CFSE expression when HLA-A2+ B cells were incubated with naïve Treg-EVs, with an overall 1.71-fold increase in mean CFSE fluorescence observed, in comparison to the control. However, similarly to the co-culture with HLA-A2- B cells, the targeted Treg-EVs showed a remarkably decreased acquisition (Figure 11b). This result was unexpected as we hoped that the post-isolation modification would significantly increase the acquisition of Treg-EVs when incubated with cells expressing the target protein, HLA-A2, in comparison with naïve human Treg-EVs.

In conclusion, post-isolation targeting of HLA-A2 antibody to PS expressed on Treg EVs did not increase their acquisition in the presence of HLA-A2. In addition, it did not overcome the lack of acquisition of Treg EVs by B cells when PS mediated acquisition was inhibited suggesting again that PS is required for Treg EV uptake in this setting.

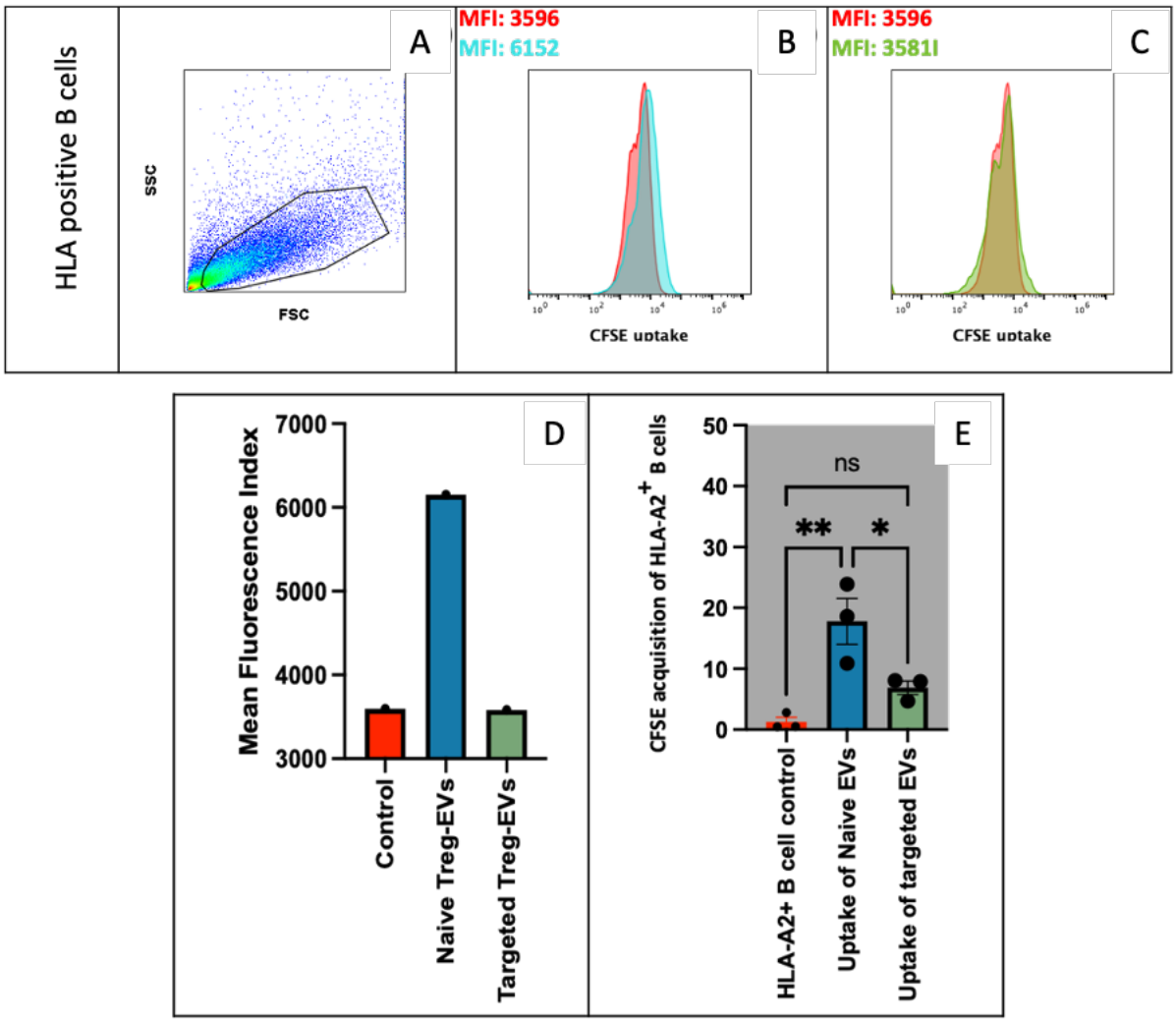

Figure 12: Acquisition of naïve and targeted Treg-EVs by HLA-A2+ B cells. The B cells in each sample, except the control were incubated at a ratio of 1 B cell with EVs isolated from 100 Tregs. A. FSC vs SSC pseudocolour plot used to gate on the expected B cell population of the expanded HLA-A2+ B cells. B. A normalised histogram overlay plot depicting CFSE expression of the B cells only control, shown in red and the HLA-A2+ B cells incubated with naïve EVs shown in dark blue, both gated on the cells shown in Figure 12a. C. A normalised histogram overlay plot of the CFSE expression of the B cells only control, shown in red and the B cells incubated with targeted Teg-EVs, shown in green, both gated on the cells gated in Figure 12a. D. Bar chart depicting the difference in MFI between control group, Naïve Treg-EV treated group and targeted Treg-EV group, n=1. E. Bar chart depicting the CFSE expression of B cells post-incubation with CFSE-labelled Treg-EVs. Each dot represents the CFSE expression of B cells analysed in three isolated uptake experiments. Data in Figure 12a-10c represents one experiment with one donor only, while Figure 12d-10e represents three isolated experiments. MFI = mean fluorescence index. ns denotes no significance between groups, * denotes a p value of <0.05 and ** denotes a p value of <0.01 as calculated using a two-way ANOVA test.

Characterisation of expanded HLA-A2 CAR Tregs

Next, we considered other EV targeting techniques, particularly pre-isolation EV modification. EVs isolated from CAR T cell have been investigated in a cancer settings (Fu *et al.*, 2019). These authors have shown CAR expression on the CAR T cell derived EVs. Furthermore, a humanised mouse model was used to show that CAR-T EVs have potent suppressive effects in inhibiting proliferation of tumour cells when compared to their parent cell. However, to my knowledge the potential of CAR-Treg derived EVs has not been investigated in a tolerance setting. To investigate this first, expanded CAR Treg cell lines were analysed for known Treg-associated proteins as well as for CAR expression using GFP, which makes up part of the CAR construct as seen in Figure 2. We found that expanded CAR Treg cell lines stably expressed GFP, thus confirming the expression of CAR on the expanded cells (Figure 13A). Expanded CAR Tregs were also shown to express CD4 and CD25, 97% and 74.4%, respectively (Figure 13B(ii) and 8B(iii)). When comparing to unstained cells, the difference in expression of GFP, CD4 and CD25 was found to be significant with very high confidence, < 0.0001 for each marker (Figure 13C(i), (ii) and(iii)).

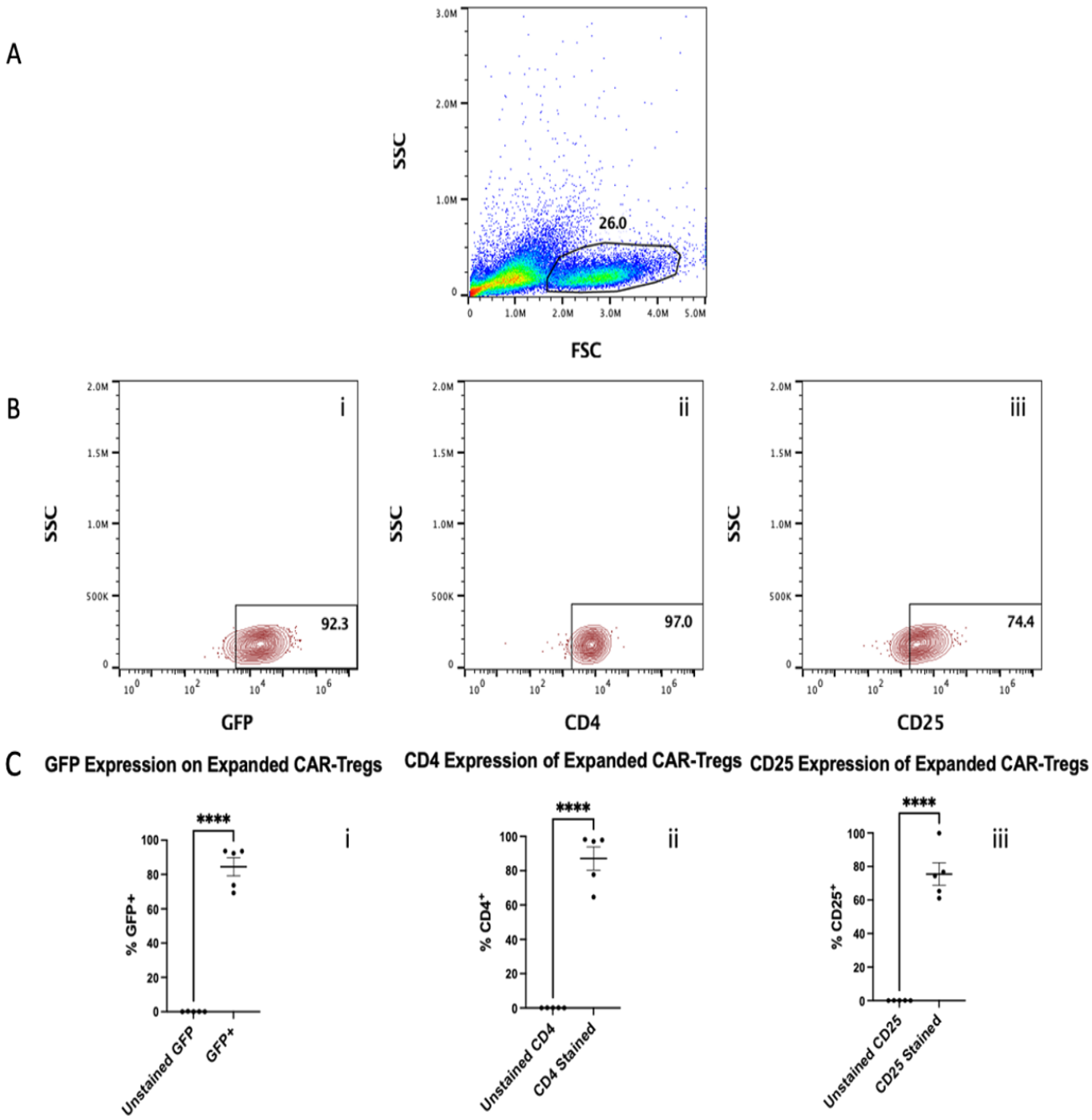
A
SSC
FSC
26.0
B
i
ii
iii
92.3
97.0
74.4
GFP
CD4
CD25
C
GFP Expression on Expanded CAR-Tregs
CD4 Expression of Expanded CAR-Tregs
CD25 Expression of Expanded CAR-Tregs
% GFP+
% CD4+
% CD25+
****
Unstained GFP
GFP+
Unstained CD4
CD4 Stained
Unstained CD25
CD25 Stained

Figure 13: Confirmation of expression of Treg cell markers on CAR Tregs. Expanded CAR Treg cells were analysed via flow cytometry to assess the expression of surface proteins commonly used to characterise Tregs. A. Dot-plot depicting the gating strategy employed to analyse the lymphocyte population in the sample using the known size and granularity of T cells. An unstained sample was then used to set gating strategy for both PE and FITC fluorescence. CD4-PE and CD25-PE-stained cells were then used to assess expression of each surface marker. B. Contour plots depictint the expression of GFP (i), CD4 (ii) and CD25(iii), (n=1). Comparative statistical analysis was carried out using a t-test to assess the significance of GFP, CD4, and CD25 expression on CAR Tregs vs the unstained cells, as shown in Figure 13c(i), Figure 13c(ii) and Figure 13c(iii), respectively. **** Denotes a P value of 0.00001<n>0.0001. Each point on Figure 13C(i)-10C(iii) represents the expression of each marker from individual expanded CAR-Treg samples. The bars show the mean +/- SD.

Treg-EVs express the HLA-A2 specific CAR

Given that CAR T cells derived EVs expressed the CAR c-Myc motif (Fu, 2019) we hypothesised that the same would be seen on CAR Treg derived EVs. To confirm this required us to find a protocol that allowed easily analyses the EVs by flow cytometry for c-Myc expression. As we had already confirmed CD81 expression of Treg-EVs using a CD81 ELISA (see Figure 8), we conceptualised a way to achieve this using anti-CD81 coated beads to capture CFSE-labelled EVs, from Exoquick isolated samples, and analyse c-Myc expression using and anti-c-Myc antibody and flow cytometry. CFSE+ Treg EVs bound to the anti-CD81 antibody coated beads, with an 8.9-fold increase in the number of EVs seen in comparison to the control sample of beads which were not incubated with EVs (Figure 14b(ii)). To further strengthen these results, the beads/EVs mixture as well as the untreated were stained with anti-CD25 antibodies. CD25 has been previously shown to be expressed on the surface of Treg-EVs (Lesley A. Smyth *et al.*, 2013; Tung *et al.*, 2020). The results showed co-expression of CFSE and CD25 on the beads (Figure 14b(iii)), and an 22-fold increase in expression in comparison to the control sample (0.00023% in the positive gate, data not shown). This data confirmed that the CD81 beads had captured the Treg-EVs. This presented an opportunity to use this protocol to confirm CAR expression on the CAR Treg-derived EVs by looking for c-Myc expression.

To this end, Treg-derived EVs from CFSE labelled CAR T cells were incubated with anti-CD81 capture beads and then stained with anti- CD25 antibody to confirm the capture of T cell derived EVs. Using unstained beads to set up gating strategies (see Figure 15b(i) an 13c(i)), the results confirmed that the CAR Treg-derived EVs were attached to the controls beads as shown in Figure 15b. There was a 660-fold increase of CD25 expression on beads incubated with Treg-EVs in comparison to CD25 stained untreated beads. Next, the presence of c-Myc was assessed. Excitingly, as shown in Figure 15c, c-Myc expression was observed on Treg-derived EVs released from CAR expressing Tregs with a 56-fold increase in c-Myc expression over control beads. In conclusion, our preliminary observations suggest that the HLA-A2 specific CAR targeting motif was expressed on the CAR-Treg derived EVs, suggesting the CAR-expressing Treg-EVs could have directed specificity to HLA-A2 expressing cells.

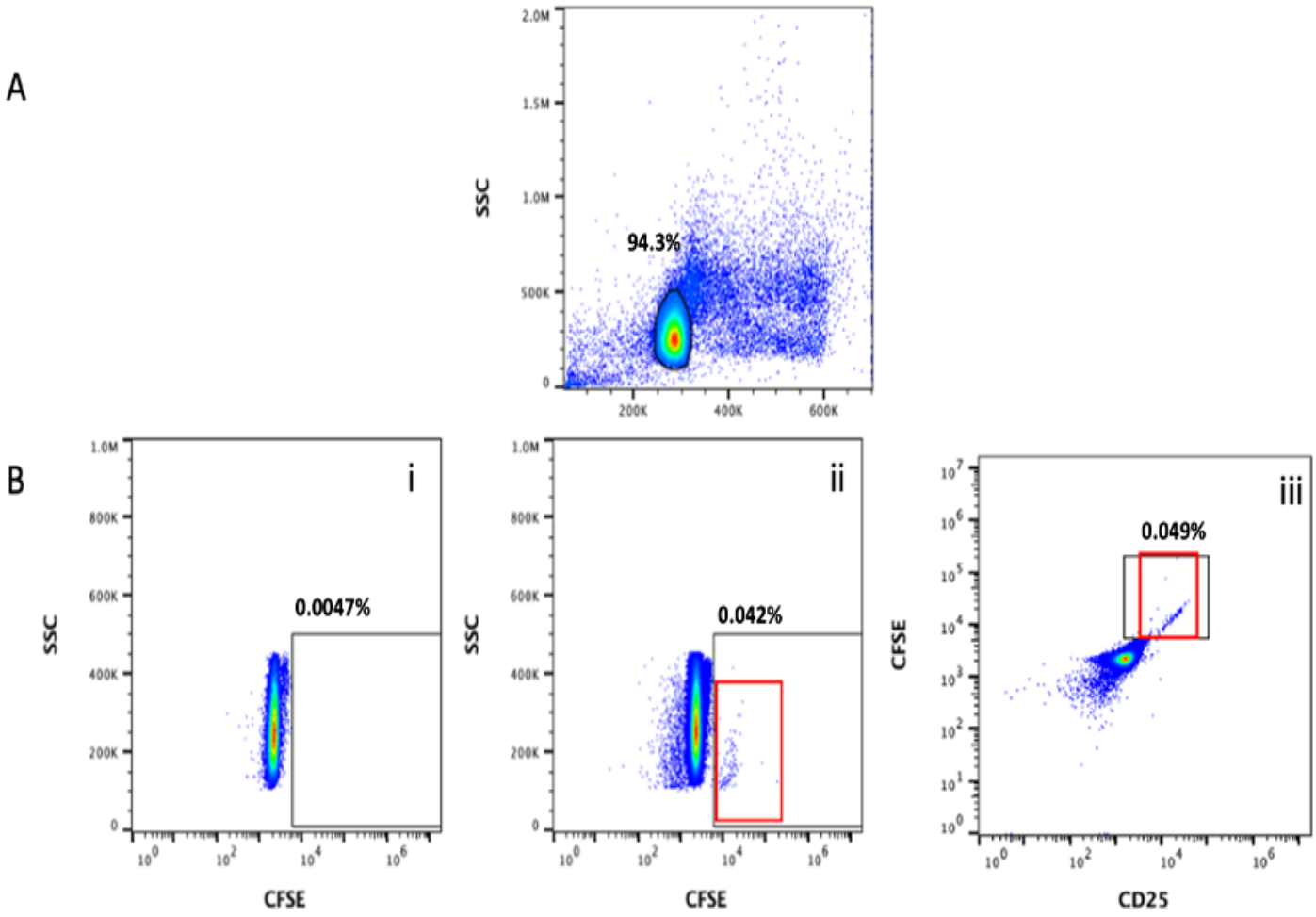

Figure 14: Treg-derived EV capture by CD81 beads.
A. Contour plot depicting the population of the CD81 beads according to their size and complexity. This gate was used to analyse CFSE and CD25 expression. B(i) is a contour plot of the control beads used to set up the gating strategy for CFSE expression. B(ii) is a contour plot depicting the CFSE expression of the beads incubated with the CFSE-labelled EVs. These CFSE expressing beads were then analysed for co-expression of CFSE and CD25b(iii) to confirm that the Treg-derived EVs had attached to the beads.

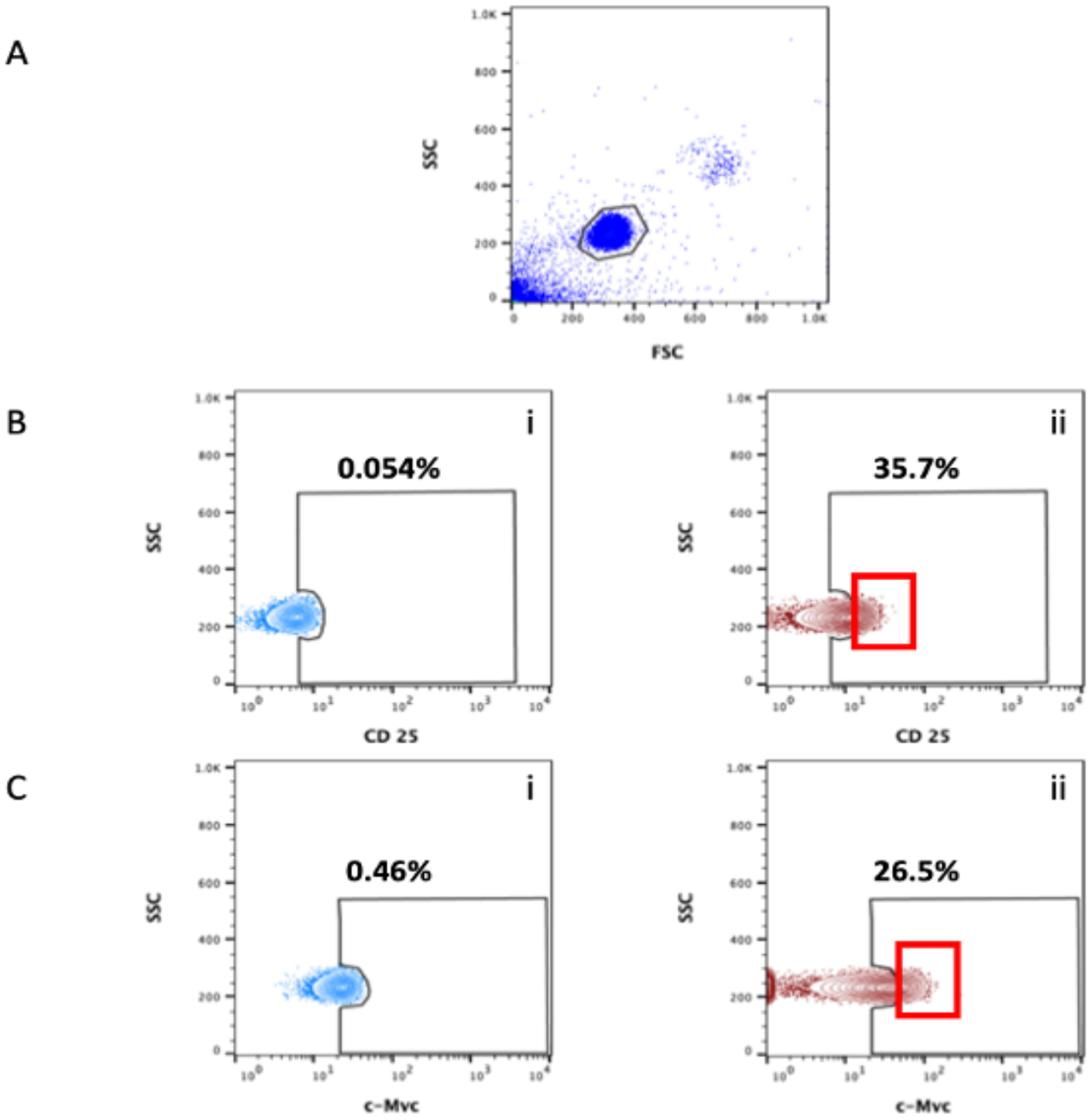

Figure 15: Validation of CAR Expression on CAR Treg-derived EVs.
Figure 15a is a dot plot depicting the population of the CD81 beads according to their size and complexity. This gate was used to analyse CD25 and c-Myc expression. Figure 15b(i) and Figure 15c(i) are contour plots of the control beads used to set up the gating strategy for CD25 and c-Myc expression, respectively. Figure 15b(ii) is a contour plot depicting the CD25 expression of the beads incubated with the CAR Treg-derived EVs. Figure 15c(ii) is a contour plot depicting the c-Myc expression of the beads incubated with the CAR Treg-derived EVs.

CAR-dependent acquisition of CAR-EVs by HLA-A2 expressing B cells

Given the aforementioned observation, that c-Myc was expressed on CAR Treg EVs, this allowing us to target pre-isolation modified EVs to HLA-A2 expressing cell lines via the HLA-A2 CAR motif. To assess the ability of B cells to acquire CAR-Treg derived EVs, EVs were harvested from the cell supernatant of activated, CFSE-labelled CAR-Treg cells and incubated with HLA-A2^{+} B cells at a ratio of 100:1, for 24 hours. CAR-Treg EVs were also incubated with HLA-A2- B cells as a control, to compare the acquisition of CAR-Treg EVs through CAR-independent means.

B cells were analysed for CFSE fluorescence using flow cytometry. As expected, CAR-Tregs were readily acquired by HLA-A2- B cells through CAR-independent means, with the number of CFSE expressing B cells increasing 6.79-fold in comparison to the non-EV treated HLA-A2- B cells, with an MFI increase of only 2.27% (Figure 16b). Comparatively, the HLA-A2+ B cells acquired slightly more EVs, with an 8.20-fold increase in CFSE expressing B cells, in comparison to the control of HLA-A2+ B cells incubated alone, with a 8.12% increase in MFI (Figure 16d). These preliminary results suggests that CAR-expression on CAR-Treg derived EVs can assist in their acquisition by cells expressing the target molecule. Statistical significance was shown between the CFSE acquisition of CAR-EV treated B cells in comparison to the control sample of B cells only (Figure 16e). Furthermore, in comparison to earlier results from this study (see Figure 10) pre-isolation modifications of EVs may result in better target specificity in comparison to EVs decorated post-isolation via PS-conjugation.

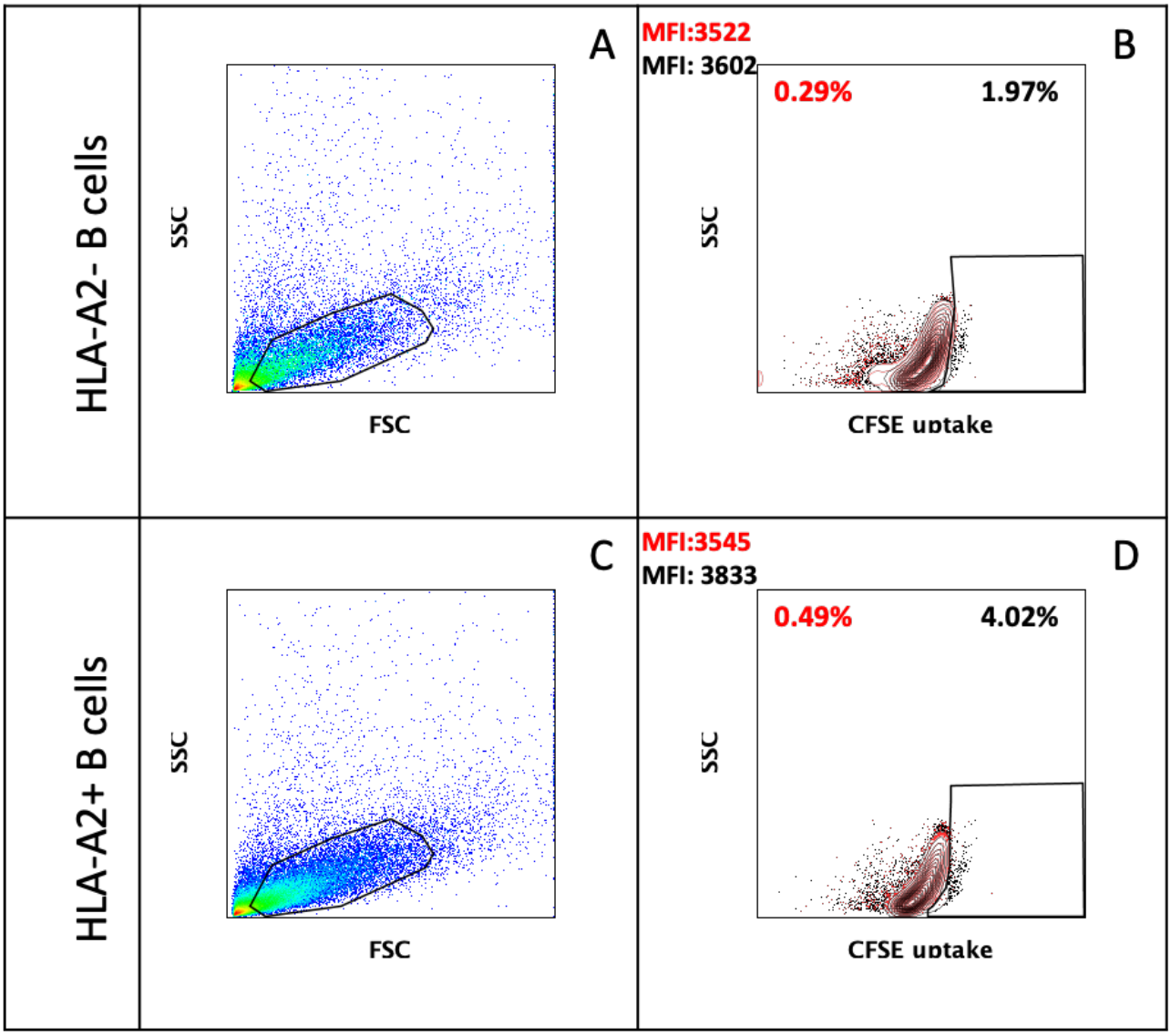
HLA-A2- B cells
A
SSC
FSC
MFI:3522
MFI: 3602
B
0.29%
1.97%
SSC
CFSE uptake
HLA-A2+ B cells
C
SSC
FSC
MFI:3545
MFI: 3833
D
0.49%
4.02%
SSC
CFSE uptake

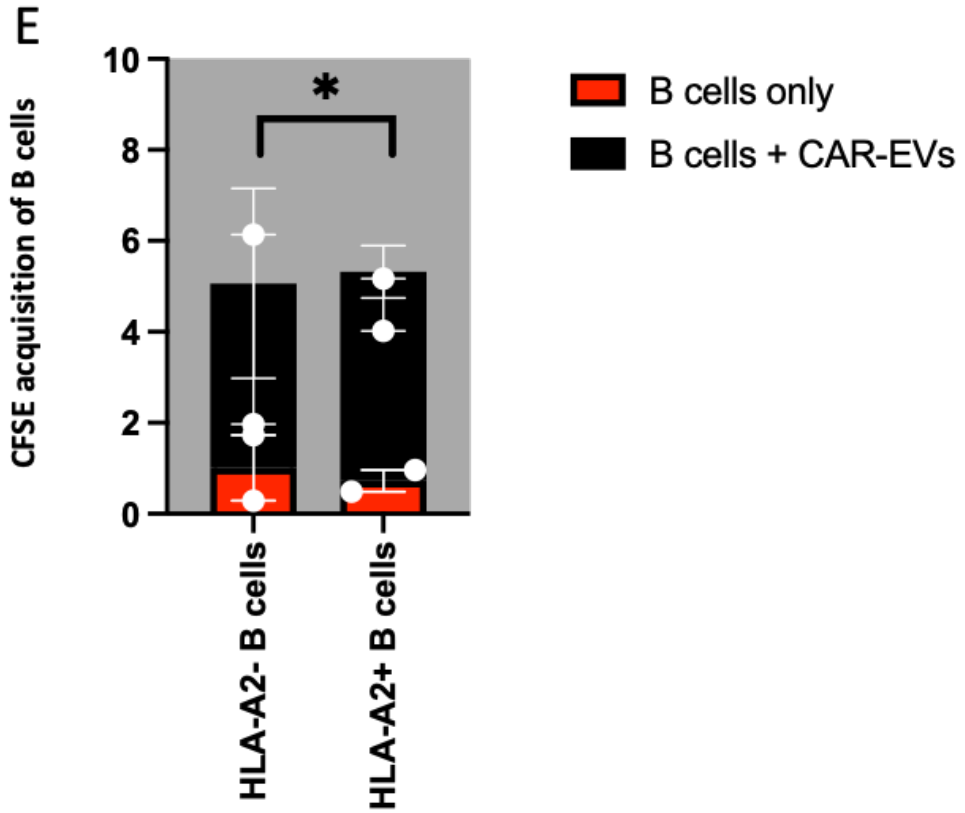

Figure 16: Acquisition of HLA-A2 CAR Treg-EVs by B cells. A. FSC vs SSC psuedocolour plot used to gate on the expected B cell population of the expanded HLA-A2- B cells. B. A contour overlay plot depicting CFSE expression of the B cells only control, shown in red and the HLA-A2- B cells incubated with CAR- EVs shown in black, both gated on the cells shown in Figure 16a. C. FSC vs SSC psuedocolour plot used to gate on the B cell population of the expanded HLA-A2+ B cells. D. A contour overlay plot depicting CFSE expression of the B cells only control, shown in red and the HLA-A2+ B cells incubated with CAR- EVs shown in black, both gated on the cells shown in Figure 44c. E. Bar chart depicting the difference in CFSE acquisition between control group and CAR-EV group, n=3. The consistent increase in CFSE acquisition was found to be significant. Data in Figure 16a-14d represents one experiment with one donor only, while 14e depicts pooled data from several independent targeting experiments. MFI = mean fluorescence index. * denotes a p value of <0.05 calculated using a one-way ANOVA.

Discussion

In this study, we aimed to engineer HLA-A2 specific Treg-EVs and assess the difference in efficacy of using pre and post-isolation targeting regimes to create antigen specific Treg-EVs. The ultimate goal is use these to induce transplant specific tolerance and promote allograft survival. For the pre-isolation modification of Treg-EVs, we indirectly targeted an anti-HLA-A2 antibody to the EVs using PS as an anchor protein on the surface of EVs and we assessed CAR-expression on EVs isolated from HLA-A2 CAR Tregs.

Tung et al., (2020) published the expression of CD63, CD81, CD25 CD39 and CCR4 on Treg EVs. Furthermore, the same authors, used proteomic screening of Treg-EVs, to confirm the expression of known EV-associated proteins including HSP90AB1, actin, tubulin as well as known EV isolation sample contaminants, serum albumin and calnexin. The authors also confirmed the size of the EVs using NanoTracking Analysis (NTA) and electron microscopy (EM). As this study utilised the Treg expansion and EV isolation protocols described in (Tung *et al.*, 2020), the Treg-EVs isolated were assumed to be similar in surface expression of these highlighted proteins.

In the study we observed that expanded $CD4^{+}CD25^{+}CD127^{lo}$ human Tregs secreted PS-expressing $CD81^{+}$ EVs that could be modified post-isolation using a PS-conjugated HLA-A2 targeting moiety. However, the acquisition of targeted Treg-EVs, measured indirectly using CFSE expression, by HLA-A2 expressing B cells was starkly decreased compared to non-modified EVs. Our preliminary results suggest that targeting post-isolation Treg EVs via PS inhibits their uptake, hinting at a possible mechanism by which Treg EVs are acquired by B cell. Contrastingly, the acquisition, of Treg-EVs expressing the HLA-A2-specific CAR is increased when it encounters the target cell *in vitro.* Taken together the possibility of using EV targeting regimes that can be exploited to increase the targeting specificity of human Tregs.

PS and Treg EV acquisition

EVs can be isolated from their parent cell using several techniques, which each have their benefits and shortcomings as reviewed by (Konoshenko *et al.*, 2018). The main isolation techniques employed are ultracentrifugation, filtration, precipitation, and affinity-based capture.

Being one of the fastest methods, ultracentrifugation is one of the most popular choices of isolation methods but involves highly specialised equipment and can cause damage to the EVs. As we did not have access to the equipment needed, although the gold standard, we could not use ultracentrifugation to isolate Treg-EVs. Filtration techniques are also popular due to its quick turnaround time and ease of use but can result in contamination or loss of sample. However, filtration techniques are constantly improving and there is now a commercial kit available which is able to isolate exosomes specifically from cell culture samples (Li *et al.*, 2017).

However, due to the lack of standardisation in isolation methods, each research group employs their own protocol, resulting in poor ability to form comparisons between studies carried out by different research groups. We have previously shown that using an ExoQuick precipitation method is a cheap, quick and effective way to reliably isolate functional EVs from the supernatant of activated immune cells, including Tregs (Tung *et al.*, 2018, 2020; Becker *et al.*, 2021). However, it has been reported that precipitation methods such as ExoQuick often lead to impure samples as reviewed by Zhao *et al.*, (2021).

In Tung et al., (2020) the authors demonstrated that human Treg-EVs isolated using ExoQuick were able to suppress T cell proliferation in vitro, modulate the cytokine profile of Teffs, potentially through the transfer of microRNAs (mi-RNAs) as well as protect allografts in vivo through the acquisition of Treg-EVs by peripheral blood mononuclear cells (PBMCs). Furthermore, a lot of the newer high-tech isolation techniques such as immunoaffinity capture rely on tags which are not readily available. Thus, considering the ease of using ExoQuick as well as ease in scaling, we decided to continue using this isolation method in this study. Using this method, we were able to isolate CD81+EVs from both CAR and non-CAR human Tregs.

Once isolated, confirming the expression of PS on human Treg-EVs was of utmost important to achieve post-isolation modifications to the EVs, making them HLA-A2 specific. PS was chosen as an anchor protein as it has been shown to be expressed in EVs isolated from several sources including platelets, tumour cells, B cells, Mast cells, human T cells and DCs (Wubbolts *et al.*, 2003; Laulagnier *et al.*, 2004; Morelli *et al.*, 2004; Zakharova, Svetlova and Fomina, 2007; Lea *et al.*, 2017; Fendl *et al.*, 2018; Lalic-Cosic *et al.*, 2021). However, to our knowledge, no literature has commented on PS expression on human Treg-EVs.

In this study we, for the first time to our knowledge, demonstrate the expression of PS on the surface of human Treg-EVs. Thus, the confirmation of surface expression of PS on Treg-derived EVs presents a novel finding and may suggest that PS expression is not limited to the EVs derived from the aforementioned sources only. This finding allowed for the confidence in direct targeting of the EVs to HLA-A2+ cells using PS as the anchor surface molecule for the targeting structure similar to what is described by (Kooijmans *et al.*, 2018) in a cancer setting but instead using a post-isolation modification method to target EVs to HLA-A2 expressing cells. In contrast to our study, Kooijmans *et al*., (2018) used the variable region of the heavy chain of an anti-EGFR antibody (Ega1). Nevertheless, portions of antibodies, such as single-chain variable fragments (scFv) have been reported to have lower binding affinity to the target than the antibody itself, often requiring further engineering to increase this (Chen *et al.*, 2019).

The distribution of internal or external phospholipid expression is believed to be controlled through the effect of intracellular calcium ions on flippase, floppase and scramblase enzymes within cells (Turturici *et al.*, 2014). Consistent with this knowledge, our results show that the expression of PS on Treg-EVs varied between isolated EVs derived from different expanded Treg samples. However, PS expression may be higher than our results indicate. The ELISA method used was dependent on the premise that isolated EVs express CD63, a well-reported EV-associated protein often used in conjunction with CD81 and CD9 to characterise EVs (Théry *et al.*, 2018). Therefore, although interesting, our results can only be used to quantify PS expression on CD63+ EVs in our sample, and this feature of the ELISA was thus used to indirectly assess the CD63 expression of isolated Treg-EVs. However, CD63 has also been shown to vary between independently isolated Treg-EV samples (Tung *et al.*, 2020). This may also be the cause of the variability of PS expression seen in this study. To address this, PS expression on Treg-EVs could have been confirmed using the aforementioned EV bead isolation protocol and subsequentially staining with PSVue, which has been shown to confirm PS expression on the surface of EVs in multiple studies (Scott-Hewitt *et al.*, 2020; Bhatta *et al.*, 2021). This will allow the expression of PS to be measured independently and more accurately, rather than through co-expression of another EV-associated protein. Furthermore, NanoFACS also presents a way to assess expression of proteins on EVs (Morales-Kastresana *et al.*, 2019) and could be used to assess PS expression on Treg-EVs. Similarly and consistent with reported results by Tung *et al*., (2020), CD81 expression on the isolated Treg-EVs also varied between samples.

Using a HLA-A2- B cell line, we also showed that B cells acquire naïve Treg-EVs without requiring specific targeting of the EVs to a surface protein expressed on B cells. Similarly, naïve Treg-EVs were also shown to be acquired by HLA-A2+ B cells. Our data show that there was a decrease in acquisition of naïve Treg-EVs that had been PS targeted in the absence of HLA-A2 expressing cells. This was in line with our hypothesis, as we believed that targeting of the EVs could potentially limit the off-target interactions with HLA-A2- cells. However, unexpectedly, a similar, but more drastic decrease in acquisition was seen when targeted Treg-EV were incubated with the target, HLA-A2 expressing cells. In this sample, the use of the CFSE expression of B cells incubated with EVs derived from CFSE-labelled Tregs, indicated that Treg-EVs were not acquired as the MFI was virtually identical to the MFI of the control sample of untreated B cells. This result was interesting and directly disproved our hypothesis which was the ability to use PS as an anchor for a targeting moiety.

PS has been described to play a role in the interaction between EVs and cells and this interaction is assumed to play a major role in the acquisition of EVs. In vitro data by Wei et al., (2016) showed that the acquisition of hypoxia-induced stem-cell derived EVs by human umbilical cord endothelial cells (HUVEC) occurs in a PS-dependent manner and was shown to be inhibited by the conjugation of PS with Annexin V. Similarly, Matsumoto et al., (2017) described macrophages acquisition of EVs via direct interaction with PS expressed on the surface of murine melanoma cell derived EVs. Using Annexin-V, Matsumoto et al., (2017) were also able to show that the direct conjugation of Annexin-V to EV surface expressed PS inhibited the acquisition of the EVs by macrophages. Similarly, the PS expressed on Treg-EVs could be conjugated with Annexin-V as shown by (Matsumoto *et al.*, 2017) and then incubated with B cells to assess the inhibition of Treg-EV acquisition by B cells due to PS 'masking' using flow cytometry.

Contrarily, (Fendl *et al.*, 2018) showed that platelet-derived EVs bound to monocytes and granulocytes in a Ca^{+} dependent but PS-independent manner and further showing that masking of PS, using Annexin V, expressed on the surface of platelet-derived EVs did not impede their binding to monocytes and granulocytes. These contrasting studies, suggest that acquisition mechanisms may be unique to the system used, thus PS could be involved in the acquisition of Treg-EVs by B cells, similarly to its role in the acquisition of melanoma cell-derived EVs by macrophages and stem cell-derived EVs by endothelial cells.

PS can be recognised and bind to several receptors expressed on various cells as reviewed by Naeini et al., (2020). One receptor molecule that can bind PS is T cell Ig and mucin domain-containing molecule 1 (TIM-1), which has been shown to be expressed on murine B cells post B cell receptor (BCR) mediated activation (Wong *et al.*, 2010). Ding et al., (2011) further showed that TIM-1 is expressed by murine regulatory B cells (Bregs) which prolong allograft survival through the expression of TIM-1 and the secretion of IL-4 and IL-10 in an islet transplant mouse model for diabetic settings. The expression of TIM-1 on human B cells was also confirmed by Aravena et al., (2017) where the authors show the ability of TIM-1 expressing B cells to inhibit CD4+ T cell responses and supress T cells in a manner distinct from transitional B cells. This highlights the possibility of the expression of TIM-1 on the surface of B cells, which may be playing a role in the acquisition of PS-expressing Treg-EVs. To investigate this possibility, similarly to (Wong *et al.*, 2010; Aravena *et al.*, 2017) an anti-TIM-1 antibody could be used to confirm the expression of TIM-1 on expanded B cells vial flow cytometry. Taken together, this suggests that B cells acquire EVs via the interaction between B cell express TIM-1 and EV expressed PS.

This elucidation of the inhibition of acquisition of Treg-EVs can be used in a cancer setting where Treg-EVs have been shown to suppress the action of cytotoxic T cells on tumour cells as described by Seo et al., (2018). Using a molecule such as X-Stamp Pro shown in this study or Annexin-V shown in (Matsumoto *et al.*, 2017), PS expressed on the surface of Treg-EVs could be 'masked', thus leading to the prevention of the role of Treg-EVs in the inhibition of cytotoxic T cell (CTL) generation in tumour microenvironments and overall promoting CTL-mediated tumour cell death.

Alternative Methods of Post Isolation EV Modifications

Although PS targeting of Treg EVs post isolation did not lead to antigen specific EVs, several other possibilities to create these EVs exist. One of the ways that has been shown to be successful is a method called Click Chemistry. Click chemistry involves the chemical process of azide alkyne cycloaddition, catalysed by copper. This allows the direct binding of small molecules onto the surface of EVs using covalent bonds as shown by (Smyth *et al.*, 2014; Wang *et al.*, 2015).

This method has been shown in (Tian *et al.*, 2018) to modify mesenchymal stromal cell-derived exosomes to express c(RGDyK) which has a high affinity to integrin in cerebral expressed in reactive cerebral vascular endothelial cells after ischemia, allowing the targeting of lesions of ischemic brains. However, as reviewed in (Ouyang *et al.*, 2018), the use of copper as the catalyst has been shown to be cytotoxic when used both *in* vitro and *in* vivo. The toxic effects of excess copper has been shown to cause oxidative damage to biological systems and proteins in humans resulting in neurological disorders, hepatitis and kidney disease (Tisato *et al.*, 2009).Other studies have shown that lipids and sugars, once cationised, are able to directly integrate into the EV surface, following direct incubation with EVs as shown by (Nakase and Futaki, 2015; Tamura, Uemoto and Tabata, 2017; Tian *et al.*, 2018). Further direct incubation methods have shown to be successful, most notably using streptavidin conjugated to DMPE-PEG which can directly integrate with EV surface (Antes *et al.*, 2018). This study also showed that the exosomes that underwent post-isolation modifications were equally as effective as the exosomes derived from pre-isolation modifications, but the overall methodology was more economical and suggested that there was a better therapeutic potential as using the 'cloaking' technique, any commercially available biotinylated antibody could be used as a targeting motif. This exponentially increases the number of potential targets of the modified exosomes. Using confocal microscopy, Kim *et al*., (2018) showed that exosomes that undergo post-isolation modifications to increase targeting specificity, localised in greater numbers in the target cell than exosomes which were not targeted. The researchers investigated the ability of bone marrow macrophage-derived exosomes to target pulmonary metastases by targeting the sigma receptor which is overexpressed by lung cancer cells, through the expression of an aminoethylanisamide-PEG peptide on the surface of the exosomes (Kim *et al.*, 2018). It has also been shown that the expression of PEG on the surface of exosomes increased circulation time from 10 minutes for unmodified exosomes, to 60 minutes for the PEG decorated exosomes (S.A.A. Kooijmans *et al.*, 2016). Similarly to the study by (Stickney *et al.*, 2016), it has been shown that CD63, a common EV marker can be modified to express a peptide, namely CP05, which via an amide linkage could be used to target specific cells such as muscle cells as shown by (Gao *et al.*, 2018). The study showed that the expression of CP05 did not alter any exosomal characteristics nor the EVs' *in vivo* distribution. Furthermore, it showed that the abundance of CD63 found in the EVs allowed for the successful dual modifications of the exosomes. Given that CD63 is an EV marker, commonly assayed across EVs derived from virtually all cell types, this method of exosomal modifications has

significant therapeutic and diagnostic potential in various settings. This is especially important for Tregs exosomes, for which investigations of their targeting potential have not been thoroughly investigated. This suggests that other receptors on the surface of EVs could be used to anchor targeting motif. To find an appropriate receptor to exploit a proteomic screen of Treg-EVs in conjunction with proteomic library data of EVs could be used to highlight expression of surface proteins. Using the knowledge in literature about the role of the proteins expressed on the surface of Treg-EVs will aid in choosing a protein that is not involved in acquisition or desired function of Treg-EVs. This could then be confirmed as through the comparison of both acquisition and function of naïve Treg-EVs and targeted EVs, similar to the experiments in this study and Tung *et al*., (2020).

Pre-Isolation method of Treg EV targeting.

(Kooijmans *et al.*, 2018) described a method of using PS expressed on the surface of EVs as an anchor for a targeting moiety to Epidermal Growth Factor Receptor EGFR expressing cells through transfection of the parent HEK293 cells. These targeted EVs were then shown to be preferentially acquired by EGFR expressing cells in a mixture of both $EGFR^+$ and $EGFR^-$ cells. Given that our results show increased acquisition of CAR-EVs by HLA-A2+ B cells, coupled with negligible acquisition of CAR-EVs by HLA-$A2^-$ B cells, a similar experiment could be used to confirm the preferential acquisition of CAR-EVs by HLA-$A2^+$ B cells, thus strengthening our new hypothesis that CAR-EVs have superior targeting specificity than directly targeted Treg-EVs.

CAR EVs have been shown to have therapeutic effect in cancer settings as described by Haque and Vaiselbuh, (2021) and Fu *et al*., (2019) who both isolated EVs using ultracentrifugation. These studies were able to confirm the expression of CAR on their parent cells using GFP and c-Myc, respectively. In our studies we confirmed the expression of CAR on EVs isolated from expanded CAR Treg cell lines, using CD81 bead isolation and the expression of the CAR motif using c-Myc, an intracellular portion of the CAR motif, similar to methods employed by Haque and Vaiselbuh, (2021). However, Fu *et al*., (2019) confirmed CAR expression on EVs by capture ELISA using EGFR constant fragment (Fc) or HER2 Fc and confirming attachment using an anti-Myc antibody and a HRP secondary antibody.

Although our method has been shown to reliably confirm the presence of CAR on EVs it may have been useful to also employ techniques such as microscale thermophoresis (MST) could be used to further validate the level of CAR expression on EVs derived from CAR-Tregs as well as confirm the interaction of EV-expressed HLA-A2 targeting CAR to HLA-A2 expressed on the target cell. This would elucidate the binding mechanism between the targeting motif and the target as well as the strength of the association. Furthermore, this technique could also be used to highlight the role of PS in the acquisition of Treg-EVs. This method has previously been used to identify miRNA cargo of EVs without the need for extraction (Zhao *et al.*, 2020) as well as to confirm the expression of PD-L1 on EVs isolated from transfected human non-small cell lung cancer cells (Huang *et al.*, 2020).

Our preliminary results show that the HLA-A2 specific CAR-Treg derived EVs were acquired more readily than naïve Treg-EVs in the presence of HLA-A2. The acquisition of CAR-Treg derived EVs however was not at remarkable levels. This may be due to the precipitation method of EV isolation used which although leads to EV recovery, also leads to heterogeneity of the EV sample as well as non-EV protein contaminants (Tang *et al.*, 2017) which could impact the EV: target cell ratio. It could prove beneficial for a second purification step to be used to purify CAR-Treg EVs to isolate a homogenous sample, which may increase the overall acquisition of CAR-EVs. This could be achieved by bead-isolation similar to the protocol used to analyse EVs using flow cytometry as previously described or using ExoQuick Ultra, which allows for a second purification step using a column (Fang *et al.*, 2021). The number of Treg-EVs needed to be acquired by the target cell in order to exert its function is unclear and Tung *et al.*, (2020) showed that naïve human Treg-EVs were suppressive, but not to the level as Tregs themselves. The level of immunosuppressive function could be heightened by using CAR Treg-EVs and this was not investigated within this study. To confirm this, a suppression assay using CAR-EVs as well as Tregs would be useful to elucidate whether increasing the targeting specificity of Treg-EVs will make their immunosuppressive effects comparable to Tregs themselves. This method could also be used to assess the difference in suppression of different target cells such as DCs and Teffs, both of which are implicated in allorecognition.

However, B cells were chosen as the target for this system due to the role B cells play in transplant rejection via the production of antibodies raised against alloantigen and the presentation of antigen to CD4+ T cells, leading to sustained T cell activation in transplant settings (Kim, 2018; Schmitz *et al.*, 2020).

Antigen specific Treg EVs as a possible therapeutic reagent

Human Treg-EVs have been described to exert immunosuppressive effects, like the Tregs themselves, in a human skin transplant setting, therefore the use of targeted Treg-EVs present a promising opportunity to inhibit allograft rejection and increase the efficacy of these vesicles. Targeting Treg-EVs to alloantigen expressing cells present in the transplanted tissue could induce accumulation of Treg-EVs at the allograft site, inhibiting immune responses from HLA-mismatch induced rejection, thus leading to allograft survival. This preferential accumulation of HLA-A2 targeted CAR-EVs to HLA-A2+ sites could be investigated by the incubation of CAR-EVs with a heterogenous sample containing equal amounts of HLA-A2+ cells and HLA-A2- cells to assess whether the CAR-EVs preferentially bind to HLA-A2+ cells. This is noteworthy as CAR-Tregs have been shown to be functionally superior in comparison to polyclonal Tregs (Tang *et al.*, 2004; Tsang *et al.*, 2008; Putnam *et al.*, 2013; Boardman *et al.*, 2017b; Kim *et al.*, 2018). Thus, there is reason to believe that like their parent cells, CAR-EVs may be functionally superior to naïve Treg-EVs as EVs have been shown to encapsulate comparable functional molecules to their parent cells in an effort to exert similar function. Similar to the *in vivo* investigation by Tung *et al*., (2020), the *in vivo* function of CAR-EVs in a transplant setting could be investigated using a similar humanised mouse xenograft model through the intravenous injection of CAR-EVs concurrently with CD4+CD25- T cells. Following this, further histological analysis to assess alloantigen damage by Teffs could be used to confirm whether, like Tregs, CAR expressing Treg-EVs promote allograft tolerance.

Current investigation into improved immunotherapies in transplant settings such as CAR-T Cell therapy has largely been stifled by the heterogeneity of Treg isolates as well as the need for ex-vivo expansion of Tregs in order to produce a therapeutically viable dose. These limitations have generated interest for using non-cellular vehicles to deliver similar functional effects. This presents an opportunity to use CAR- EVs, the non-cellular counterparts of CAR-

Tregs, as a potential solution and reducing the requirement for ex vivo expansion of the therapeutic product as well as potentially decreasing the functional dose of EVs administered.

CAR-EVs could also be used as a targeted delivery system that can delivery specific cargo, such as miRNA to target cells as shown by (Tung *et al.*, 2020). EVs can be loaded with specific cargo to deliver to target cells through direct incorporation of exogenous cargo using methods such as electroporation, sonication or incubation or through the exploitation of protein or RNA sorting machinery after transfection of the parent cell as reviewed by (Elsharkasy *et al.*, 2020). Investigations could also be made using proteomics to identify the cargo naturally encapsulated by Treg-EVs and highlight the potential involvement of the cargo in the immunomodulatory nature of Treg-EVs.

Overall, this study is limited to a proof of concept due to the limited number of independently repeated experiments largely caused by the difficulty in expanding Treg cell lines as opposed to primary Treg cell cultures. Furthermore, it is difficult to compare this study to other research in the field because of the lack of explicit characterisation according to the standards set by the ISEV (Witwer *et al.*, 2021) to define subsets of EVs. There is also a lack of quantification which, if known, could inform discussions surrounding the number of Treg-EVs required to achieve a remarked effect in the target cells which is useful to the future of this research area and could justify the use of Treg-EVs instead of their cellular counterparts.

Future works

This study has laid the foundation for further study into the potential of pre-isolation modified Treg-EVs in the field of transplantation and leads to research into how to further increase targeting efficiency of Treg-EVs through the expression of CAR motifs raised against HLA-A2 expressing cells. By optimising the Treg expansion protocol, we would have the opportunity to elucidate the suppressive effects of EVs on the target B cells, using a suppression assay. It would also be interesting to study the potential use of preventing EV acquisition via PS by blocking its interaction with PS-receptors. To achieve this, we could study acquisition of 'PS-blocked EVs', EVs which do not express surface PS and naïve EVs using fluorescence microscopy; allowing us to further shed light on the theorised role of PS in EV acquisition.

Conclusion

This study highlights that human Treg-EVs, like EVs derived from several other sources, express PS which may play a role in the acquisition of Treg-EVs. This was suggested when the post-isolation modification of EV-expressing PS, via conjugation with a PS targeting motif, inhibited acquisition of Treg-EVs by B cells. This observation informs on how Treg EVs are acquired which has yet to be elucidated, it also suggests that conjugation of PS may inhibit the acquisition of Treg-EVs which could potentially be exploited in a cancer setting to prevent cytotoxic T cell suppression via Treg-EVs. On the other hand, using a pre-isolation modification of Tregs, to express an HLA-A2 targeting CAR, this study delivered preliminary data showing expression of CAR on EVs isolated from CAR-Tregs, and that these EVs were acquired by B cells expressing the CAR specific antigen, HLA-A2. This suggests the potential for CAR-EVs to be used to target HLA expressing cells and promote allograft tolerance through the inhibition of HLA-mismatched graft rejection pathways.

References.

Agarwal, A. *et al.* (2014) 'Regulatory T Cell-Derived Exosomes: Possible Therapeutic and Diagnostic Tools in Transplantation', *Frontiers in Immunology*, 5. Available at: https://doi.org/10.3389/fimmu.2014.00555.

Aiello, S. *et al.* (2017) 'Extracellular vesicles derived from T regulatory cells suppress T cell proliferation and prolong allograft survival', *Scientific Reports*, 7(1), p. 11518. Available at: https://doi.org/10.1038/s41598-017-08617-3.

Akkaya, B. *et al.* (2019) 'Regulatory T cells mediate specific suppression by depleting peptide–MHC class II from dendritic cells', *Nature Immunology*, 20(2), pp. 218–231. Available at: https://doi.org/10.1038/s41590-018-0280-2.

Alvarez-Erviti, L. *et al.* (2011) 'Delivery of siRNA to the mouse brain by systemic injection of targeted exosomes', *Nature Biotechnology*, 29(4), pp. 341–345. Available at: https://doi.org/10.1038/nbt.1807.

Amini, L. *et al.* (2021) 'Super-Treg: Toward a New Era of Adoptive Treg Therapy Enabled by Genetic Modifications', *Frontiers in Immunology*, 11, p. 611638. Available at: https://doi.org/10.3389/fimmu.2020.611638.

Andersen, M.H. *et al.* (2000) 'Functional Analyses of Two Cellular Binding Domains of Bovine Lactadherin', *Biochemistry*, 39(20), pp. 6200–6206. Available at: https://doi.org/10.1021/bi992221r.

Antes, T.J. *et al.* (2018) 'Targeting extracellular vesicles to injured tissue using membrane cloaking and surface display', *Journal of Nanobiotechnology*, 16(1), p. 61. Available at: https://doi.org/10.1186/s12951-018-0388-4.

Aravena, O. *et al.* (2017) 'TIM-1 defines a human regulatory B cell population that is altered in frequency and function in systemic sclerosis patients', *Arthritis Research & Therapy*, 19(1), p. 8. Available at: https://doi.org/10.1186/s13075-016-1213-9.

Azuma, T. *et al.* (2003) 'Human CD4+ CD25+ regulatory T cells suppress NKT cell functions', *Cancer Research*, 63(15), pp. 4516–4520.

Ballke, C. *et al.* (2016) 'Characterization of Regulatory T-Cell Markers in CD4+ T Cells of the Upper Airway Mucosa', *PLOS ONE*. Edited by D. Unutmaz, 11(2), p. e0148826. Available at: https://doi.org/10.1371/journal.pone.0148826.

Barao, I. *et al.* (2006) 'Suppression of natural killer cell-mediated bone marrow cell rejection by CD4 $^{+}$ CD25 $^{+}$ regulatory T cells', *Proceedings of the National Academy of Sciences*, 103(14), pp. 5460–5465. Available at: https://doi.org/10.1073/pnas.0509249103.

Becker, P.D. *et al.* (2021) 'B lymphocytes contribute to indirect pathway T cell sensitization via acquisition of extracellular vesicles', *American Journal of Transplantation*, 21(4), pp. 1415–1426. Available at: https://doi.org/10.1111/ajt.16088.

Bettini, M.L. and Vignali, D.A.A. (2010) 'Development of thymically derived natural regulatory T cells: Development of thymically derived nTregs', *Annals of the New York Academy of Sciences*, 1183(1), pp. 1–12. Available at: https://doi.org/10.1111/j.1749-6632.2009.05129.x.

Bhatta, M. *et al.* (2021) 'Novel phosphatidylserine-binding molecule enhances antitumor T-cell responses by targeting immunosuppressive exosomes in human tumor microenvironments', *Journal for ImmunoTherapy of Cancer*, 9(10), p. e003148. Available at: https://doi.org/10.1136/jitc-2021-003148.

Blanchard, N. *et al.* (2002) 'TCR Activation of Human T Cells Induces the Production of Exosomes Bearing the TCR/CD3/ζ Complex', *The Journal of Immunology*, 168(7), pp. 3235–3241. Available at: https://doi.org/10.4049/jimmunol.168.7.3235.

Bluestone, J.A. *et al.* (2015) 'Type 1 diabetes immunotherapy using polyclonal regulatory T cells', *Science Translational Medicine*, 7(315). Available at: https://doi.org/10.1126/scitranslmed.aad4134.

Boardman, D.A. *et al.* (2017) 'Expression of a Chimeric Antigen Receptor Specific for Donor HLA Class I Enhances the Potency of Human Regulatory T Cells in Preventing Human Skin Transplant Rejection', *American Journal of Transplantation*, 17(4), pp. 931–943. Available at: https://doi.org/10.1111/ajt.14185.6

Boroughs, A.C. *et al.* (2019) 'Chimeric antigen receptor costimulation domains modulate human regulatory T cell function', *JCI Insight*, 4(8), p. e126194. Available at: https://doi.org/10.1172/jci.insight.126194.

Brook, M.O. *et al.* (2022) 'Transplantation Without Overimmunosuppression (TWO) study protocol: a phase 2b randomised controlled single-centre trial of regulatory T cell therapy to facilitate immunosuppression reduction in living donor kidney transplant recipients', *BMJ Open*, 12(4), p. e061864. Available at: https://doi.org/10.1136/bmjopen-2022-061864.

Campos-Mora, M. *et al.* (2019) 'CD4+Foxp3+T Regulatory Cells Promote Transplantation Tolerance by Modulating Effector CD4+ T Cells in a Neuropilin-1-Dependent Manner', *Frontiers in Immunology*, 10, p. 882. Available at: https://doi.org/10.3389/fimmu.2019.00882.

Chaput, N. (2006) 'Dendritic cell derived-exosomes: biology and clinical implementations', *Journal of Leukocyte Biology*, 80(3), pp. 471–478. Available at: https://doi.org/10.1189/jlb.0206094.

Chen, Q. *et al.* (2019) 'Affinity improvement of the fully human anti-TSLP recombinant antibody', *Molecular Medicine Reports* [Preprint]. Available at: https://doi.org/10.3892/mmr.2019.10880.

Collison, L.W. *et al.* (2009) 'Regulatory T Cell Suppression Is Potentiated by Target T Cells in a Cell Contact, IL-35- and IL-10-Dependent Manner', *The Journal of Immunology*, 182(10), pp. 6121–6128. Available at: https://doi.org/10.4049/jimmunol.0803646.

Colombo, M. *et al.* (2013) 'Analysis of ESCRT functions in exosome biogenesis, composition and secretion highlights the heterogeneity of extracellular vesicles', *Journal of Cell Science*, p. jcs.128868. Available at: https://doi.org/10.1242/jcs.128868.

Delcayre, A. *et al.* (2005) 'Exosome Display technology: Applications to the development of new diagnostics and therapeutics', *Blood Cells, Molecules, and Diseases*, 35(2), pp. 158–168. Available at: https://doi.org/10.1016/j.bcmd.2005.07.003.

Ding, Q. *et al.* (2011) 'Regulatory B cells are identified by expression of TIM-1 and can be induced through TIM-1 ligation to promote tolerance in mice', *Journal of Clinical Investigation*, 121(9), pp. 3645–3656. Available at: https://doi.org/10.1172/JCI46274.

DiPaolo, R.J. *et al.* (2007) 'Autoantigen-Specific TGFβ-Induced Foxp3 $^{+}$ Regulatory T Cells Prevent Autoimmunity by Inhibiting Dendritic Cells from Activating Autoreactive T Cells', *The Journal of Immunology*, 179(7), pp. 4685–4693. Available at: https://doi.org/10.4049/jimmunol.179.7.4685.

Dowling, M.R. *et al.* (2018) 'Regulatory T Cells Suppress Effector T Cell Proliferation by Limiting Division Destiny', *Frontiers in Immunology*, 9, p. 2461. Available at: https://doi.org/10.3389/fimmu.2018.02461.

Doyle, L. and Wang, M. (2019) 'Overview of Extracellular Vesicles, Their Origin, Composition, Purpose, and Methods for Exosome Isolation and Analysis', *Cells*, 8(7), p. 727. Available at: https://doi.org/10.3390/cells8070727.

Elsharkasy, O.M. *et al.* (2020) 'Extracellular vesicles as drug delivery systems: Why and how?', *Advanced Drug Delivery Reviews*, 159, pp. 332–343. Available at: https://doi.org/10.1016/j.addr.2020.04.004.

Ernst, P.B., Garrison, J.C. and Thompson, L.F. (2010) 'Much Ado about Adenosine: Adenosine Synthesis and Function in Regulatory T Cell Biology', *The Journal of Immunology*, 185(4), pp. 1993–1998. Available at: https://doi.org/10.4049/jimmunol.1000108.

Fang, X. *et al.* (2021) 'A magnetic bead-mediated selective adsorption strategy for extracellular vesicle separation and purification', *Acta Biomaterialia*, 124, pp. 336–347. Available at: https://doi.org/10.1016/j.actbio.2021.02.004.

Fassbender, M. *et al.* (2010) 'Cyclic adenosine monophosphate and IL-10 coordinately contribute to nTreg cell-mediated suppression of dendritic cell activation', *Cellular Immunology*, 265(2), pp. 91–96. Available at: https://doi.org/10.1016/j.cellimm.2010.07.007.

Fendl, B. *et al.* (2018) 'Differential Interaction of Platelet-Derived Extracellular Vesicles With Circulating Immune Cells: Roles of TAM Receptors, CD11b, and Phosphatidylserine', *Frontiers in Immunology*, 9, p. 2797. Available at: https://doi.org/10.3389/fimmu.2018.02797.

Fu, W. *et al.* (2019) 'CAR exosomes derived from effector CAR-T cells have potent antitumour effects and low toxicity', *Nature Communications*, 10(1), p. 4355. Available at: https://doi.org/10.1038/s41467-019-12321-3.

Gao, X. *et al.* (2018) 'Anchor peptide captures, targets, and loads exosomes of diverse origins for diagnostics and therapy', *Science Translational Medicine*, 10(444), p. eaat0195. Available at: https://doi.org/10.1126/scitranslmed.aat0195.

Golshayan, D. *et al.* (2007) 'In vitro–expanded donor alloantigen–specific CD4+CD25+ regulatory T cells promote experimental transplantation tolerance', *Blood*, 109(2), pp. 827–835. Available at: https://doi.org/10.1182/blood-2006-05-025460.

Gondek, D.C. *et al.* (2005) 'Cutting Edge: Contact-Mediated Suppression by $CD4^+$ $CD25^+$ Regulatory Cells Involves a Granzyme B-Dependent, Perforin-Independent Mechanism', *The Journal of Immunology*, 174(4), pp. 1783–1786. Available at: https://doi.org/10.4049/jimmunol.174.4.1783.

Ha, D., Yang, N. and Nadithe, V. (2016) 'Exosomes as therapeutic drug carriers and delivery vehicles across biological membranes: current perspectives and future challenges', *Acta Pharmaceutica Sinica B*, 6(4), pp. 287–296. Available at: https://doi.org/10.1016/j.apsb.2016.02.001.

Haque, S. and Vaiselbuh, S.R. (2021) 'CD19 Chimeric Antigen Receptor-Exosome Targets CD19 Positive B-lineage Acute Lymphocytic Leukemia and Induces Cytotoxicity', *Cancers*, 13(6), p. 1401. Available at: https://doi.org/10.3390/cancers13061401.

Harden, P.N. *et al.* (2021) 'Feasibility, long-term safety, and immune monitoring of regulatory T cell therapy in living donor kidney transplant recipients', *American Journal of Transplantation*, 21(4), pp. 1603–1611. Available at: https://doi.org/10.1111/ajt.16395.

Hartman, Z.C. *et al.* (2011) 'Increasing vaccine potency through exosome antigen targeting', *Vaccine*, 29(50), pp. 9361–9367. Available at: https://doi.org/10.1016/j.vaccine.2011.09.133.

Hippen, K.L. *et al.* (2011) 'Massive ex Vivo Expansion of Human Natural Regulatory T Cells (T_{regs}) with Minimal Loss of in Vivo Functional Activity', *Science Translational Medicine*, 3(83). Available at: https://doi.org/10.1126/scitranslmed.3001809.

Hori, S., Nomura, T. and Sakaguchi, S. (2003) 'Control of Regulatory T Cell Development by the Transcription Factor *Foxp3*', *Science*, 299(5609), pp. 1057–1061. Available at: https://doi.org/10.1126/science.1079490.

Hosseini, A. *et al.* (2016) 'Exosome-inspired targeting of cancer cells with enhanced affinity', *Journal of Materials Chemistry B*, 4(4), pp. 768–778. Available at: https://doi.org/10.1039/C5TB01741F.

Huang, M. *et al.* (2020) 'Homogeneous, Low-volume, Efficient, and Sensitive Quantitation of Circulating Exosomal PD-L1 for Cancer Diagnosis and Immunotherapy Response Prediction',

Angewandte Chemie International Edition, 59(12), pp. 4800–4805. Available at: https://doi.org/10.1002/anie.201916039.

Issa, F. *et al.* (2019) 'Transiently Activated Human Regulatory T Cells Upregulate BCL-XL Expression and Acquire a Functional Advantage in vivo', *Frontiers in Immunology*, 10, p. 889. Available at: https://doi.org/10.3389/fimmu.2019.00889.

Ius, F. *et al.* (2019) 'Five-Year Results of an IgA and IgM-Enriched Human Immunoglobulin G-Based Therapy for Early Anti-HLA Donor Specific Antibodies in 158 Lung-Transplanted Patients', *The Journal of Heart and Lung Transplantation*, 38(4), p. S166. Available at: https://doi.org/10.1016/j.healun.2019.01.398.

Joffre, O. *et al.* (2008) 'Prevention of acute and chronic allograft rejection with CD4+CD25+Foxp3+ regulatory T lymphocytes', *Nature Medicine*, 14(1), pp. 88–92. Available at: https://doi.org/10.1038/nm1688.

Jonuleit, H. *et al.* (2001) 'Identification and Functional Characterization of Human Cd4+Cd25+ T Cells with Regulatory Properties Isolated from Peripheral Blood', *Journal of Experimental Medicine*, 193(11), pp. 1285–1294. Available at: https://doi.org/10.1084/jem.193.11.1285.

Kakarla, R. *et al.* (2020) 'Apoptotic cell-derived exosomes: messages from dying cells', *Experimental & Molecular Medicine*, 52(1), pp. 1–6. Available at: https://doi.org/10.1038/s12276-019-0362-8.

Kanamori, M. *et al.* (2016) 'Induced Regulatory T Cells: Their Development, Stability, and Applications', *Trends in Immunology*, 37(11), pp. 803–811. Available at: https://doi.org/10.1016/j.it.2016.08.012.

Kato, Z. *et al.* (2008) 'Positioning of autoimmune TCR-Ob.2F3 and TCR-Ob.3D1 on the MBP85–99/HLA-DR2 complex', *Proceedings of the National Academy of Sciences*, 105(40), pp. 15523–15528. Available at: https://doi.org/10.1073/pnas.0807338105.

Kim, M.S. *et al.* (2018) 'Engineering macrophage-derived exosomes for targeted paclitaxel delivery to pulmonary metastases: in vitro and in vivo evaluations', *Nanomedicine: Nanotechnology, Biology and Medicine*, 14(1), pp. 195–204. Available at: https://doi.org/10.1016/j.nano.2017.09.011.

Kim, T.J. (2018) 'The Role of B Cells in Transplantation Rejection', *The Journal of the Korean Society for Transplantation*, 32(1), p. 1. Available at: https://doi.org/10.4285/jkstn.2018.32.1.1.

Kim, Y.C. *et al.* (2015) 'Engineered antigen-specific human regulatory T cells: immunosuppression of FVIII-specific T- and B-cell responses', *Blood*, 125(7), pp. 1107–1115. Available at: https://doi.org/10.1182/blood-2014-04-566786.

Konoshenko, M.Yu. *et al.* (2018) 'Isolation of Extracellular Vesicles: General Methodologies and Latest Trends', *BioMed Research International*, 2018, pp. 1–27. Available at: https://doi.org/10.1155/2018/8545347.

Kooijmans, Sander A. A. *et al.* (2016) 'Display of GPI-anchored anti-EGFR nanobodies on extracellular vesicles promotes tumour cell targeting', *Journal of Extracellular Vesicles*, 5(1), p. 31053. Available at: https://doi.org/10.3402/jev.v5.31053.

Kooijmans, S.A.A. *et al.* (2016) 'PEGylated and targeted extracellular vesicles display enhanced cell specificity and circulation time', *Journal of Controlled Release*, 224, pp. 77–85. Available at: https://doi.org/10.1016/j.jconrel.2016.01.009.

Kooijmans, S.A.A. *et al.* (2018) 'Recombinant phosphatidylserine-binding nanobodies for targeting of extracellular vesicles to tumor cells: a plug-and-play approach', *Nanoscale*, 10(5), pp. 2413–2426. Available at: https://doi.org/10.1039/C7NR06966A.

Lalic-Cosic, S. *et al.* (2021) 'Phosphatidylserine Exposing Extracellular Vesicles in Pre-eclamptic Patients', *Frontiers in Medicine*, 8, p. 761453. Available at: https://doi.org/10.3389/fmed.2021.761453.

Lam, A.J. *et al.* (2022) 'Helios is a marker, not a driver, of human Treg stability', *European Journal of Immunology*, 52(1), pp. 75–84. Available at: https://doi.org/10.1002/eji.202149318.

Lara, P. *et al.* (2020) 'Exploiting the Natural Properties of Extracellular Vesicles in Targeted Delivery towards Specific Cells and Tissues', *Pharmaceutics*, 12(11), p. 1022. Available at: https://doi.org/10.3390/pharmaceutics12111022.

Laulagnier, K. *et al.* (2004) 'Mast cell- and dendritic cell-derived exosomes display a specific lipid composition and an unusual membrane organization', *Biochemical Journal*, 380(1), pp. 161–171. Available at: https://doi.org/10.1042/bj20031594.

Lea, J. *et al.* (2017) 'Detection of phosphatidylserine-positive exosomes as a diagnostic marker for ovarian malignancies: a proof of concept study', *Oncotarget*, 8(9), pp. 14395–14407. Available at: https://doi.org/10.18632/oncotarget.14795.

Li, P. *et al.* (2017) 'Progress in Exosome Isolation Techniques', *Theranostics*, 7(3), pp. 789–804. Available at: https://doi.org/10.7150/thno.18133.

Liao, F., Lu, X. and Dong, W. (2020) 'Exosomes derived from T regulatory cells relieve inflammatory bowel disease by transferring MIR -195a-3p', *IUBMB Life*, 72(12), pp. 2591–2600. Available at: https://doi.org/10.1002/iub.2385.

Lim, H.W. *et al.* (2005) 'Cutting Edge: Direct Suppression of B Cells by $CD4^+$ $CD25^+$ Regulatory T Cells', *The Journal of Immunology*, 175(7), pp. 4180–4183. Available at: https://doi.org/10.4049/jimmunol.175.7.4180.

Liu, Y. *et al.* (2015) 'Targeted exosome-mediated delivery of opioid receptor Mu siRNA for the treatment of morphine relapse', *Scientific Reports*, 5(1), p. 17543. Available at: https://doi.org/10.1038/srep17543.

MacDonald, K.G. *et al.* (2016) 'Alloantigen-specific regulatory T cells generated with a chimeric antigen receptor', *Journal of Clinical Investigation*, 126(4), pp. 1413–1424. Available at: https://doi.org/10.1172/JCI82771.

Matsumoto, A. *et al.* (2017) 'Role of Phosphatidylserine-Derived Negative Surface Charges in the Recognition and Uptake of Intravenously Injected B16BL6-Derived Exosomes by Macrophages', *Journal of Pharmaceutical Sciences*, 106(1), pp. 168–175. Available at: https://doi.org/10.1016/j.xphs.2016.07.022.

Mikami, N. *et al.* (2020) 'Epigenetic conversion of conventional T cells into regulatory T cells by CD28 signal deprivation', *Proceedings of the National Academy of Sciences*, 117(22), pp. 12258–12268. Available at: https://doi.org/10.1073/pnas.1922600117.

Mohseni, Y.R. *et al.* (2021) 'Chimeric antigen receptor-modified human regulatory T cells that constitutively express IL-10 maintain their phenotype and are potently suppressive', *European Journal of Immunology*, 51(10), pp. 2522–2530. Available at: https://doi.org/10.1002/eji.202048934.

Morales-Kastresana, A. *et al.* (2019) 'High-fidelity detection and sorting of nanoscale vesicles in viral disease and cancer', *Journal of Extracellular Vesicles*, 8(1), p. 1597603. Available at: https://doi.org/10.1080/20013078.2019.1597603.

Morelli, A.E. *et al.* (2004) 'Endocytosis, intracellular sorting, and processing of exosomes by dendritic cells', *Blood*, 104(10), pp. 3257–3266. Available at: https://doi.org/10.1182/blood-2004-03-0824.

Naeini, M.B. *et al.* (2020) 'The role of phosphatidylserine recognition receptors in multiple biological functions', *Cellular & Molecular Biology Letters*, 25(1), p. 23. Available at: https://doi.org/10.1186/s11658-020-00214-z.

Nakase, I. and Futaki, S. (2015) 'Combined treatment with a pH-sensitive fusogenic peptide and cationic lipids achieves enhanced cytosolic delivery of exosomes', *Scientific Reports*, 5(1), p. 10112. Available at: https://doi.org/10.1038/srep10112.

Noyan, F. *et al.* (2017) 'Prevention of Allograft Rejection by Use of Regulatory T Cells With an MHC-Specific Chimeric Antigen Receptor', *American Journal of Transplantation*, 17(4), pp. 917–930. Available at: https://doi.org/10.1111/ajt.14175.

Oggero, S., Austin-Williams, S. and Norling, L.V. (2019) 'The Contrasting Role of Extracellular Vesicles in Vascular Inflammation and Tissue Repair', *Frontiers in Pharmacology*, 10, p. 1479. Available at: https://doi.org/10.3389/fphar.2019.01479.

Ohno, S. *et al.* (2013) 'Systemically Injected Exosomes Targeted to EGFR Deliver Antitumor MicroRNA to Breast Cancer Cells', *Molecular Therapy*, 21(1), pp. 185–191. Available at: https://doi.org/10.1038/mt.2012.180.

Okeke, E.B. and Uzonna, J.E. (2019) 'The Pivotal Role of Regulatory T Cells in the Regulation of Innate Immune Cells', *Frontiers in Immunology*, 10, p. 680. Available at: https://doi.org/10.3389/fimmu.2019.00680.

Okoye, I.S. *et al.* (2014) 'MicroRNA-Containing T-Regulatory-Cell-Derived Exosomes Suppress Pathogenic T Helper 1 Cells', *Immunity*, 41(1), pp. 89–103. Available at: https://doi.org/10.1016/j.immuni.2014.05.019.

Onishi, Y. *et al.* (2008) 'Foxp3+ natural regulatory T cells preferentially form aggregates on dendritic cells in vitro and actively inhibit their maturation', *Proceedings of the National Academy of Sciences*, 105(29), pp. 10113–10118. Available at: https://doi.org/10.1073/pnas.0711106105.

Ouyang, T. *et al.* (2018) 'Recent trends in click chemistry as a promising technology for virus-related research', *Virus Research*, 256, pp. 21–28. Available at: https://doi.org/10.1016/j.virusres.2018.08.003.

Pandiyan, P. *et al.* (2007) 'CD4+CD25+Foxp3+ regulatory T cells induce cytokine deprivation–mediated apoptosis of effector CD4+ T cells', *Nature Immunology*, 8(12), pp. 1353–1362. Available at: https://doi.org/10.1038/ni1536.

Pillai, V. *et al.* (2007) 'Transient regulatory T-cells: A state attained by all activated human T-cells', *Clinical Immunology*, 123(1), pp. 18–29. Available at: https://doi.org/10.1016/j.clim.2006.10.014.

Putnam, A.L. *et al.* (2013) 'Clinical Grade Manufacturing of Human Alloantigen-Reactive Regulatory T Cells for Use in Transplantation: Clinical Grade Alloantigen-Reactive Tregs', *American Journal of Transplantation*, 13(11), pp. 3010–3020. Available at: https://doi.org/10.1111/ajt.12433.

Raposo, G. and Stoorvogel, W. (2013) 'Extracellular vesicles: Exosomes, microvesicles, and friends', *The Journal of Cell Biology*, 200(4), pp. 373–383. Available at: https://doi.org/10.1083/jcb.201211138.

Romano, M. *et al.* (2018) 'Expanded Regulatory T Cells Induce Alternatively Activated Monocytes With a Reduced Capacity to Expand T Helper-17 Cells', *Frontiers in Immunology*, 9, p. 1625. Available at: https://doi.org/10.3389/fimmu.2018.01625.

Rountree, R.B. *et al.* (2011) 'Exosome Targeting of Tumor Antigens Expressed by Cancer Vaccines Can Improve Antigen Immunogenicity and Therapeutic Efficacy', *Cancer Research*, 71(15), pp. 5235–5244. Available at: https://doi.org/10.1158/0008-5472.CAN-10-4076.

R.Walker, M. *et al.* (2003) 'Induction of FoxP3 and acquisition of T regulatory activity by stimulated human CD4+CD25– T cells', *Journal of Clinical Investigation*, 112(9), pp. 1437–1443. Available at: https://doi.org/10.1172/JCI19441.

Sadelain, M., Brentjens, R. and Rivière, I. (2013) 'The Basic Principles of Chimeric Antigen Receptor Design', *Cancer Discovery*, 3(4), pp. 388–398. Available at: https://doi.org/10.1158/2159-8290.CD-12-0548.

Safinia, N. *et al.* (2016) 'Successful expansion of functional and stable regulatory T cells for immunotherapy in liver transplantation', *Oncotarget*, 7(7), pp. 7563–7577. Available at: https://doi.org/10.18632/oncotarget.6927.

Sagoo, P. *et al.* (2011) 'Human Regulatory T Cells with Alloantigen Specificity Are More Potent Inhibitors of Alloimmune Skin Graft Damage than Polyclonal Regulatory T Cells', *Science Translational Medicine*, 3(83). Available at: https://doi.org/10.1126/scitranslmed.3002076.

Sánchez-Fueyo, A. *et al.* (2020) 'Applicability, safety, and biological activity of regulatory T cell therapy in liver transplantation', *American Journal of Transplantation*, 20(4), pp. 1125–1136. Available at: https://doi.org/10.1111/ajt.15700.

Saunderson, S.C. *et al.* (2014) 'CD169 mediates the capture of exosomes in spleen and lymph node', *Blood*, 123(2), pp. 208–216. Available at: https://doi.org/10.1182/blood-2013-03-489732.

Sawitzki, B. *et al.* (2020) 'Regulatory cell therapy in kidney transplantation (The ONE Study): a harmonised design and analysis of seven non-randomised, single-arm, phase 1/2A trials', *The Lancet*, 395(10237), pp. 1627–1639. Available at: https://doi.org/10.1016/S0140-6736(20)30167-7.

Schmitz, R. *et al.* (2020) 'B cells in transplant tolerance and rejection: friends or foes?', *Transplant International*, 33(1), pp. 30–40. Available at: https://doi.org/10.1111/tri.13549.

Scotta, C. *et al.* (2013) 'Differential effects of rapamycin and retinoic acid on expansion, stability and suppressive qualities of human CD4+CD25+FOXP3+ T regulatory cell subpopulations', *Haematologica*, 98(8), pp. 1291–1299. Available at: https://doi.org/10.3324/haematol.2012.074088.

Scott-Hewitt, N. *et al.* (2020) 'Local externalization of phosphatidylserine mediates developmental synaptic pruning by microglia', *The EMBO Journal*, 39(16). Available at: https://doi.org/10.15252/embj.2020105380.

Seo, N., Akiyoshi, K. and Shiku, H. (2018) 'Exosome-mediated regulation of tumor immunology', *Cancer Science*, 109(10), pp. 2998–3004. Available at: https://doi.org/10.1111/cas.13735.

Sette, P. *et al.* (2010) 'The ESCRT-Associated Protein Alix Recruits the Ubiquitin Ligase Nedd4-1 To Facilitate HIV-1 Release through the LYPX $_n$ L L Domain Motif', *Journal of Virology*, 84(16), pp. 8181–8192. Available at: https://doi.org/10.1128/JVI.00634-10.

Sharma, S. *et al.* (2015) 'CD4+CD25+CD127low Regulatory T Cells Play Predominant Anti-Tumor Suppressive Role in Hepatitis B Virus-Associated Hepatocellular Carcinoma', *Frontiers in Immunology*, 6. Available at: https://doi.org/10.3389/fimmu.2015.00049.

Shigemoto-Kuroda, T. *et al.* (2017) 'MSC-derived Extracellular Vesicles Attenuate Immune Responses in Two Autoimmune Murine Models: Type 1 Diabetes and Uveoretinitis', *Stem Cell Reports*, 8(5), pp. 1214–1225. Available at: https://doi.org/10.1016/j.stemcr.2017.04.008.

Sicard, A. *et al.* (2020) 'Donor-specific chimeric antigen receptor Tregs limit rejection in naive but not sensitized allograft recipients', *American Journal of Transplantation*, 20(6), pp. 1562–1573. Available at: https://doi.org/10.1111/ajt.15787.

Smyth, Lesley Ann *et al.* (2013) 'CD73 expression on extracellular vesicles derived from CD4 $^{+}$ CD25 $^{+}$ Foxp3 $^{+}$ T cells contributes to their regulatory function: Immunomodulation', *European Journal of Immunology*, 43(9), pp. 2430–2440. Available at: https://doi.org/10.1002/eji.201242909.

Smyth, Lesley A. *et al.* (2013) 'Tolerogenic Donor-Derived Dendritic Cells Risk Sensitization In Vivo owing to Processing and Presentation by Recipient APCs', *The Journal of Immunology*, 190(9), pp. 4848–4860. Available at: https://doi.org/10.4049/jimmunol.1200870.

Smyth, T. *et al.* (2014) 'Surface Functionalization of Exosomes Using Click Chemistry', *Bioconjugate Chemistry*, 25(10), pp. 1777–1784. Available at: https://doi.org/10.1021/bc500291r.

Stephens, L.A., Malpass, K.H. and Anderton, S.M. (2009) 'Curing CNS autoimmune disease with myelin-reactive Foxp3 $^{+}$ Treg', *European Journal of Immunology*, 39(4), pp. 1108–1117. Available at: https://doi.org/10.1002/eji.200839073.

Stickney, Z. *et al.* (2016) 'Development of exosome surface display technology in living human cells', *Biochemical and Biophysical Research Communications*, 472(1), pp. 53–59. Available at: https://doi.org/10.1016/j.bbrc.2016.02.058.

Takahashi, T. *et al.* (1998) 'Immunologic self-tolerance maintained by CD25+CD4+ naturally anergic and suppressive T cells: induction of autoimmune disease by breaking their anergic/suppressive state.', *International Immunology*, 10(12), pp. 1969–1980. Available at: https://doi.org/10.1093/intimm/10.12.1969.

Tamura, R., Uemoto, S. and Tabata, Y. (2017) 'Augmented liver targeting of exosomes by surface modification with cationized pullulan', *Acta Biomaterialia*, 57, pp. 274–284. Available at: https://doi.org/10.1016/j.actbio.2017.05.013.

Tang, Q. *et al.* (2004) 'In Vitro–expanded Antigen-specific Regulatory T Cells Suppress Autoimmune Diabetes', *Journal of Experimental Medicine*, 199(11), pp. 1455–1465. Available at: https://doi.org/10.1084/jem.20040139.

Tang, Y.-T. *et al.* (2017) 'Comparison of isolation methods of exosomes and exosomal RNA from cell culture medium and serum', *International Journal of Molecular Medicine*, 40(3), pp. 834–844. Available at: https://doi.org/10.3892/ijmm.2017.3080.

Tarbell, K.V. *et al.* (2004) 'CD25+ CD4+ T Cells, Expanded with Dendritic Cells Presenting a Single Autoantigenic Peptide, Suppress Autoimmune Diabetes', *Journal of Experimental Medicine*, 199(11), pp. 1467–1477. Available at: https://doi.org/10.1084/jem.20040180.

Tekguc, M. *et al.* (2021) 'Treg-expressed CTLA-4 depletes CD80/CD86 by trogocytosis, releasing free PD-L1 on antigen-presenting cells', *Proceedings of the National Academy of Sciences*, 118(30), p. e2023739118. Available at: https://doi.org/10.1073/pnas.2023739118.

Théry, C. *et al.* (2018) 'Minimal information for studies of extracellular vesicles 2018 (MISEV2018): a position statement of the International Society for Extracellular Vesicles and update of the MISEV2014 guidelines', *Journal of Extracellular Vesicles*, 7(1), p. 1535750. Available at: https://doi.org/10.1080/20013078.2018.1535750.

Thornton, A.M. and Shevach, E.M. (1998) 'CD4+CD25+ Immunoregulatory T Cells Suppress Polyclonal T Cell Activation In Vitro by Inhibiting Interleukin 2 Production', *Journal of Experimental Medicine*, 188(2), pp. 287–296. Available at: https://doi.org/10.1084/jem.188.2.287.

Tian, T. *et al.* (2018) 'Surface functionalized exosomes as targeted drug delivery vehicles for cerebral ischemia therapy', *Biomaterials*, 150, pp. 137–149. Available at: https://doi.org/10.1016/j.biomaterials.2017.10.012.

Tisato, F. *et al.* (2009) 'Copper in diseases and treatments, and copper-based anticancer strategies', *Medicinal Research Reviews*, p. n/a-n/a. Available at: https://doi.org/10.1002/med.20174.

Todo, S. *et al.* (2016) 'A pilot study of operational tolerance with a regulatory T-cell-based cell therapy in living donor liver transplantation', *Hepatology*, 64(2), pp. 632–643. Available at: https://doi.org/10.1002/hep.28459.

Trenado, A. *et al.* (2003) 'Recipient-type specific CD4+CD25+ regulatory T cells favor immune reconstitution and control graft-versus-host disease while maintaining graft-versus-leukemia', *Journal of Clinical Investigation*, 112(11), pp. 1688–1696. Available at: https://doi.org/10.1172/JCI17702.

Tsang, J.Y.-S. *et al.* (2008) 'Conferring indirect allospecificity on CD4+CD25+ Tregs by TCR gene transfer favors transplantation tolerance in mice', *Journal of Clinical Investigation*, 118(11), pp. 3619–3628. Available at: https://doi.org/10.1172/JCI33185.

Tung, S.L. *et al.* (2018) 'Regulatory T cell-derived extracellular vesicles modify dendritic cell function', *Scientific Reports*, 8(1), p. 6065. Available at: https://doi.org/10.1038/s41598-018-24531-8.

Tung, S.L. *et al.* (2020) 'Regulatory T cell extracellular vesicles modify T-effector cell cytokine production and protect against human skin allograft damage', *Frontiers in Cell and Developmental Biology* [Preprint]. Available at: https://doi.org/10.3389/fcell.2020.00317.

Turturici, G. *et al.* (2014) 'Extracellular membrane vesicles as a mechanism of cell-to-cell communication: advantages and disadvantages', *American Journal of Physiology-Cell Physiology*, 306(7), pp. C621–C633. Available at: https://doi.org/10.1152/ajpcell.00228.2013.

Van Niel, G. *et al.* (2001) 'Intestinal epithelial cells secrete exosome–like vesicles', *Gastroenterology*, 121(2), pp. 337–349. Available at: https://doi.org/10.1053/gast.2001.26263.

Wang, J.-H. *et al.* (2018) 'Anti-HER2 scFv-Directed Extracellular Vesicle-Mediated mRNA-Based Gene Delivery Inhibits Growth of HER2-Positive Human Breast Tumor Xenografts by Prodrug Activation', *Molecular Cancer Therapeutics*, 17(5), pp. 1133–1142. Available at: https://doi.org/10.1158/1535-7163.MCT-17-0827.

Wang, M. *et al.* (2015) 'Integrating Protein Engineering and Bioorthogonal Click Conjugation for Extracellular Vesicle Modulation and Intracellular Delivery', *PLOS ONE*. Edited by R.M. Hakami, 10(11), p. e0141860. Available at: https://doi.org/10.1371/journal.pone.0141860.

Wei, X. *et al.* (2016) 'Surface Phosphatidylserine Is Responsible for the Internalization on Microvesicles Derived from Hypoxia-Induced Human Bone Marrow Mesenchymal Stem Cells into Human Endothelial Cells', *PLOS ONE*. Edited by G. Camussi, 11(1), p. e0147360. Available at: https://doi.org/10.1371/journal.pone.0147360.

Wiklander, O.P.B. *et al.* (2015) 'Extracellular vesicle in vivo biodistribution is determined by cell source, route of administration and targeting', *Journal of Extracellular Vesicles*, 4(1), p. 26316. Available at: https://doi.org/10.3402/jev.v4.26316.

Witwer, K.W. *et al.* (2021) 'Updating MISEV: Evolving the minimal requirements for studies of extracellular vesicles', *Journal of Extracellular Vesicles*, 10(14). Available at: https://doi.org/10.1002/jev2.12182.

Wolfers, J. *et al.* (2001) 'Tumor-derived exosomes are a source of shared tumor rejection antigens for CTL cross-priming', *Nature Medicine*, 7(3), pp. 297–303. Available at: https://doi.org/10.1038/85438.

Wong, S.H. *et al.* (2010) 'Tim-1 is induced on germinal centre B cells through B-cell receptor signalling but is not essential for the germinal centre response: Tim-1 is up-regulated on germinal centre B cells', *Immunology*, p. no-no. Available at: https://doi.org/10.1111/j.1365-2567.2010.03276.x.

Wubbolts, R. *et al.* (2003) 'Proteomic and Biochemical Analyses of Human B Cell-derived Exosomes', *Journal of Biological Chemistry*, 278(13), pp. 10963–10972. Available at: https://doi.org/10.1074/jbc.M207550200.

Xu, A. *et al.* (2016) 'TGF-β–Induced Regulatory T Cells Directly Suppress B Cell Responses through a Noncytotoxic Mechanism', *The Journal of Immunology*, 196(9), pp. 3631–3641. Available at: https://doi.org/10.4049/jimmunol.1501740.

Ye, J. *et al.* (2012) 'Human regulatory T cells induce T-lymphocyte senescence', *Blood*, 120(10), pp. 2021–2031. Available at: https://doi.org/10.1182/blood-2012-03-416040.

Yeo, R.W.Y. *et al.* (2013) 'Mesenchymal stem cell: An efficient mass producer of exosomes for drug delivery', *Advanced Drug Delivery Reviews*, 65(3), pp. 336–341. Available at: https://doi.org/10.1016/j.addr.2012.07.001.

Yu, X. *et al.* (2013) 'CD4+CD25+ regulatory T cells-derived exosomes prolonged kidney allograft survival in a rat model', *Cellular Immunology*, 285(1–2), pp. 62–68. Available at: https://doi.org/10.1016/j.cellimm.2013.06.010.

Yuen-Shan Tsang, J. *et al.* (2009) 'Indefinite mouse heart allograft survival in recipient treated with CD4+CD25+ regulatory T cells with indirect allospecificity and short term immunosuppression', *Transplant Immunology*, 21(4), pp. 203–209. Available at: https://doi.org/10.1016/j.trim.2009.05.003.

Zaborowski, M.P. *et al.* (2015) 'Extracellular Vesicles: Composition, Biological Relevance, and Methods of Study', *BioScience*, 65(8), pp. 783–797. Available at: https://doi.org/10.1093/biosci/biv084.

Zakharova, L., Svetlova, M. and Fomina, A.F. (2007) 'T cell exosomes induce cholesterol accumulation in human monocytes via phosphatidylserine receptor', *Journal of Cellular Physiology*, 212(1), pp. 174–181. Available at: https://doi.org/10.1002/jcp.21013.

Zhao, H., Liao, X. and Kang, Y. (2017) 'Tregs: Where We Are and What Comes Next?', *Frontiers in Immunology*, 8, p. 1578. Available at: https://doi.org/10.3389/fimmu.2017.01578.

Zhao, J. *et al.* (2020) 'Thermophoretic Detection of Exosomal microRNAs by Nanoflares', *Journal of the American Chemical Society*, 142(11), pp. 4996–5001. Available at: https://doi.org/10.1021/jacs.9b13960.

Zhao, Z. *et al.* (2021) 'Isolation and analysis methods of extracellular vesicles (EVs)', *Extracellular Vesicles and Circulating Nucleic Acids* [Preprint]. Available at: https://doi.org/10.20517/evcna.2021.07.

Zitvogel, L. *et al.* (1998) 'Eradication of established murine tumors using a novel cell-free vaccine: dendritic cell derived exosomes', *Nature Medicine*, 4(5), pp. 594–600. Available at: https://doi.org/10.1038/nm0598-594.

Appendix

Appendix 1: A table listing the supplier information for the reagents used in this study.

Reagent/Equipment	Gifted by	Supplier Information
Eppendorf 5920R centrifuge	NA	ThermoFisher, Paisley, UK
Pen-Strep	Dr Marco Romano, KCL	
EV-Free FCS	NA	
L-glutamine		
CD3/CD28 Expansion beads	Dr Marco Romano, KCL	
Biolite 24 well multi-dish plate	NA	
DynaMag-15 Magnetic Separator	NA	
Trypan Blue	NA	
PBS	NA	
96 U-bottom well plate	NA	
CFSE	NA	
anti-CD3	NA	
anti-CD28	Dr Sim Tung, KCL	
CD81-Dynabeads	NA	
Micro-BCA Protein Assay Kit	NA	
0.22µm filter	NA	Miltenyi, Surrey, UK
ExoQuick	NA	SystemBiosciences, Colne, UK
CD81 ExoELISA	NA	
X-Stamp Pro-Streptavidin	NA	
PS Exosome-Capture ELISA	NA	Alpha Laboratories, Eastleigh, UK

Appendix 2: A table listing the supplier information and clones for the antibodies used in this study.

Antibody	Conjugated Fluorochrome	Clone	Supplier Information
anti-CD4	PE	OKT-4	ThermoFisher, Paisley, UK
anti-CD25	PE	BC96	
anti-CD127	FITC	eBioRDR5	
HLA-A2	PE	REAFINITY	Miltenyi, Surrey, UK
HLA-A2	Biotin		
anti-c-Myc	Alexa Fluor 594	9E10	Biolegend, London, UK